PEM Fuel Cells

and the

Role of Nanomorphology in Polymer Electrolytes

CDNA – Jan. 31, 2008

Bruce Balcom	MRI & Physics	University New Brunswick
Greg Baker	Chemistry	Michigan State University
Keith Promislow	Mathematics	Michigan State University
Hang Zhang	Mathematics	Michigan State University

Talk Overview

I) Fuel Cells for dummies
II) Scientific Overview
    - Components
    - Macroscopic Unit Cell Models
III) Pore Formation in Polymer Electrolytes
    - Nanoscale Issues
    - Prior Computataional Approaches
    - CPE equations
    - Comparison to data
    - Impact on proton conduction
IV) Nanophase Models
    - Catalyst Layer Macroscale Models Nanoscale Preparation
    - Greg Swain's Membranes
    - Pt dissolution

I) PEMFC for Dummies: Energy Effeciency

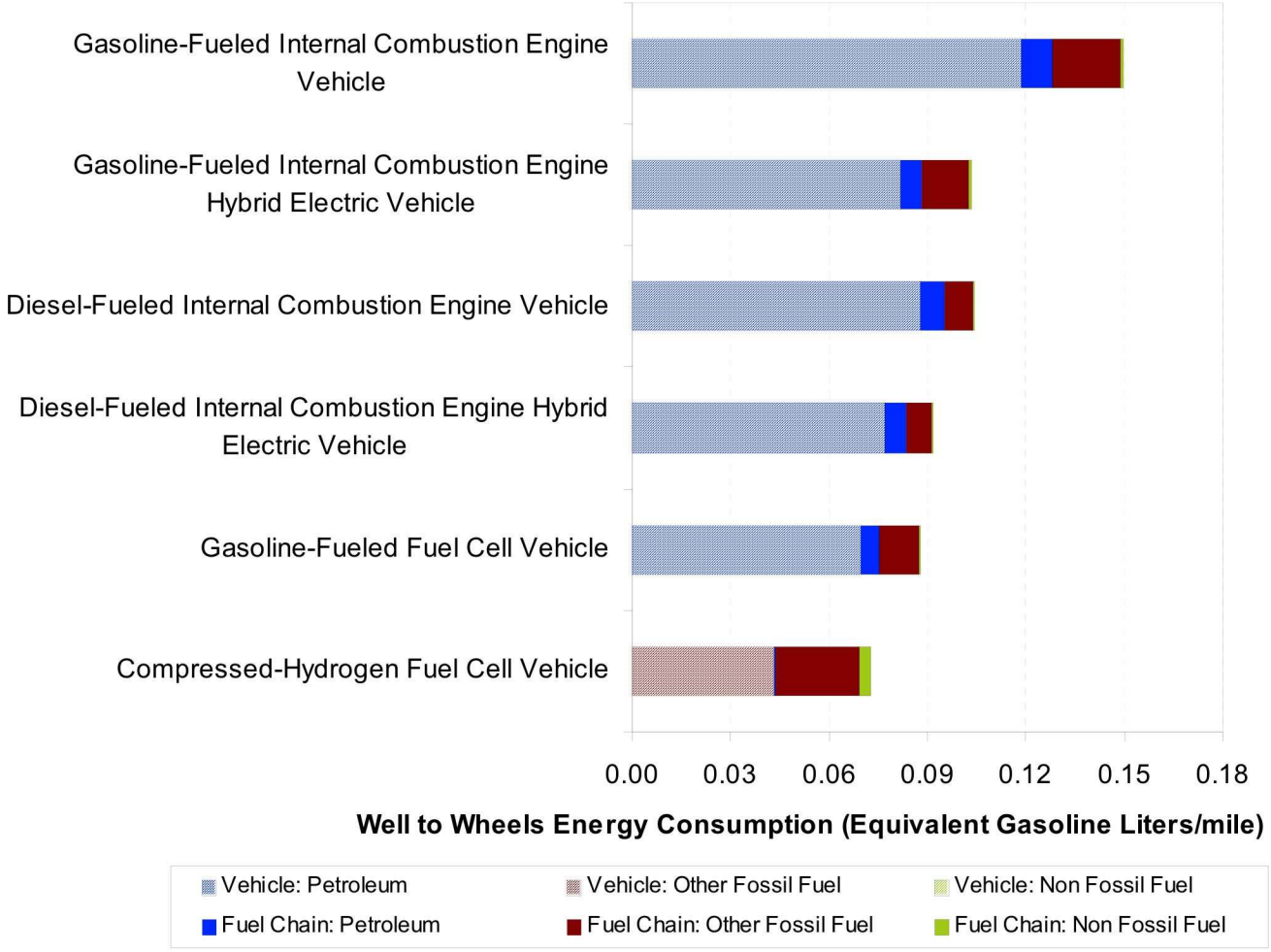

Source: ADL-DOE Fuel Choice for Fuel Cell Vehicles Study Results, February 2002

How Much Energy?

1 lb of Fat	3000 Calories
1 Gallon Gasoline	30,000 Calories
1 Kw-hour	0.28 lb Fat
80 MPH @ 20 MPG	40 lbs Fat/hour
My house with AC running	1.25 lbs Fat/hour
US daily gasoline consumption	2000 Calories per day per person in world
US annual gasoline consumption	20 $\times$ US annual corn production
40 Miles @ 20 MPG	40 bags Tostedos corn chips

PEM Fuel Cell: Macroview

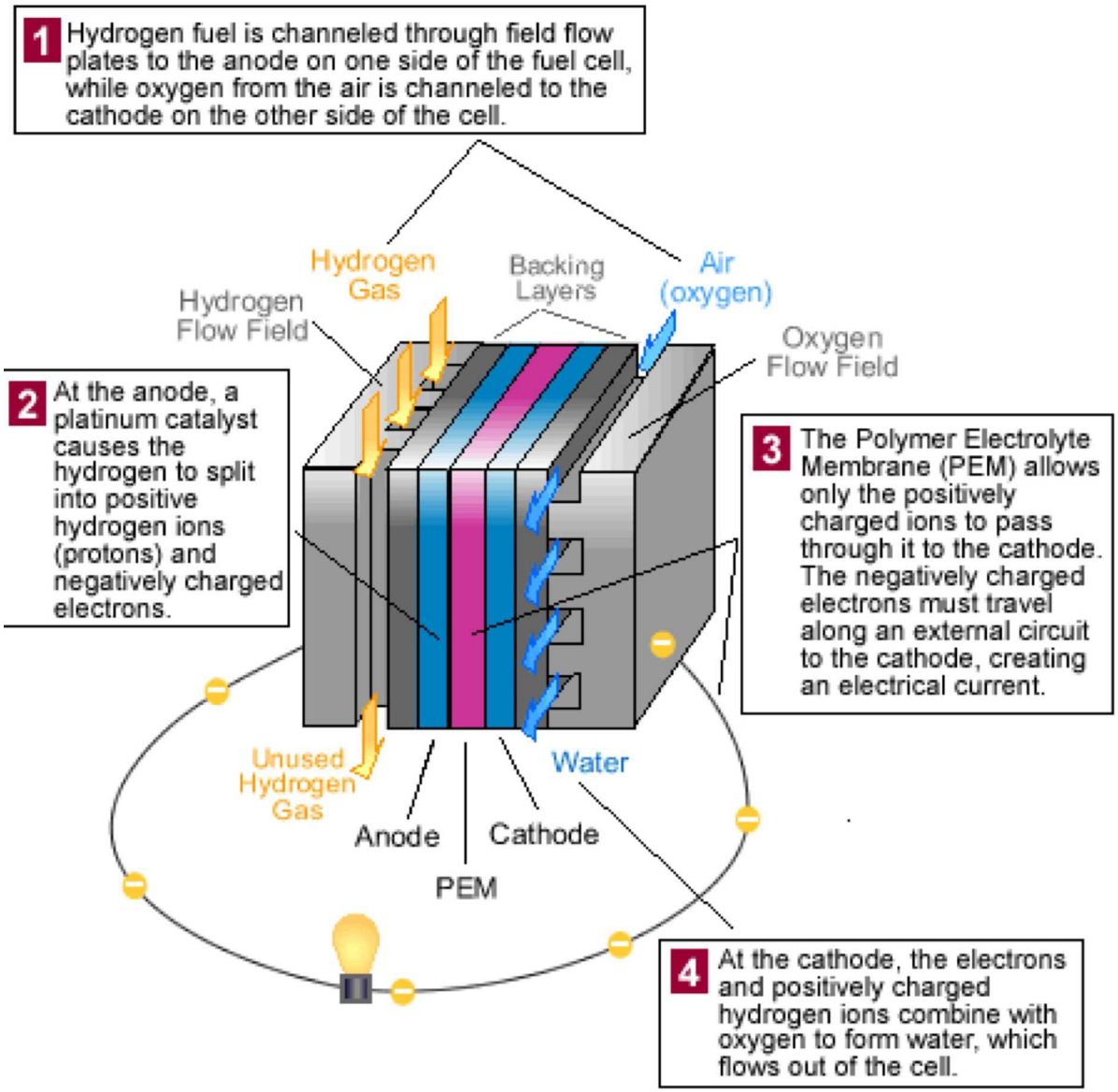

A Bit More Detail

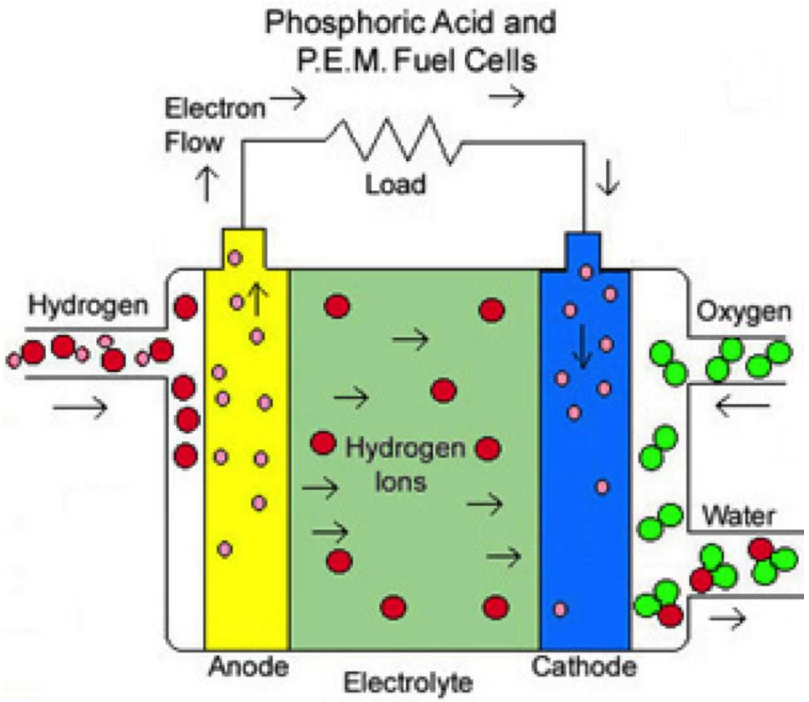

$$2H_2 + O_2 \rightarrow 2H_2O + 1.2V$$

Volts = Energy/electron

This is the WRONG reaction

Opps

NanoPotatoes in PEM Fuel Cells

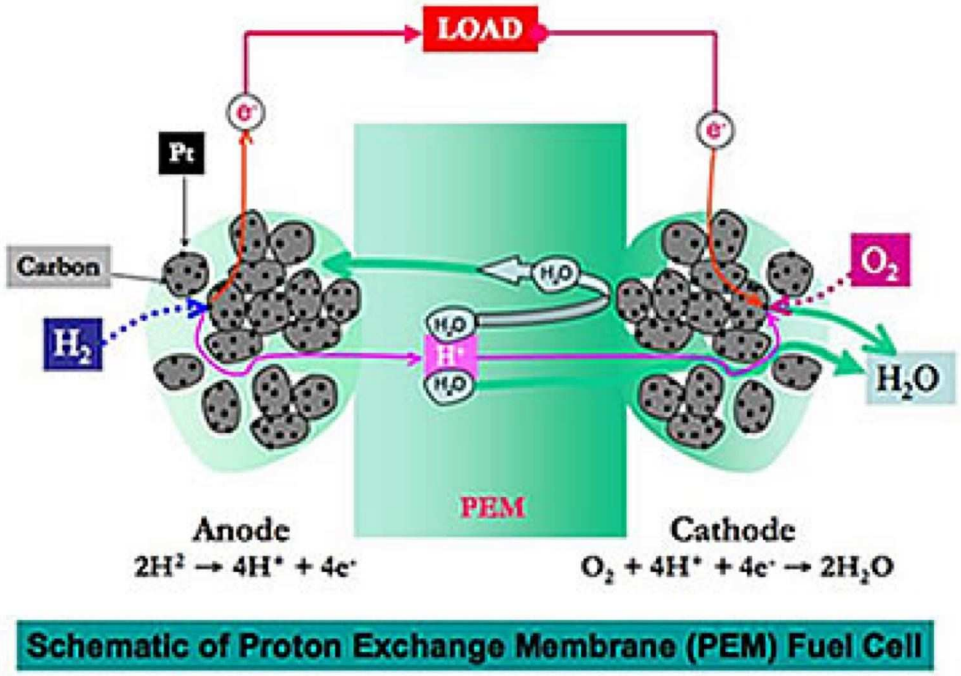

Schematic of Proton Exchange Membrane (PEM) Fuel Cell

$H_2 \rightarrow_{\mathrm{Pt}} 2H^+ + 2e^-$

Hydrogen Oxidation Reaction

$4H^+ + 4e^- + O_2 \rightarrow_{\mathrm{Pt}} 2H_2O + \mathrm{Heat}$

Oxygen Reduction Reaction

Other Types of Fuel Cells

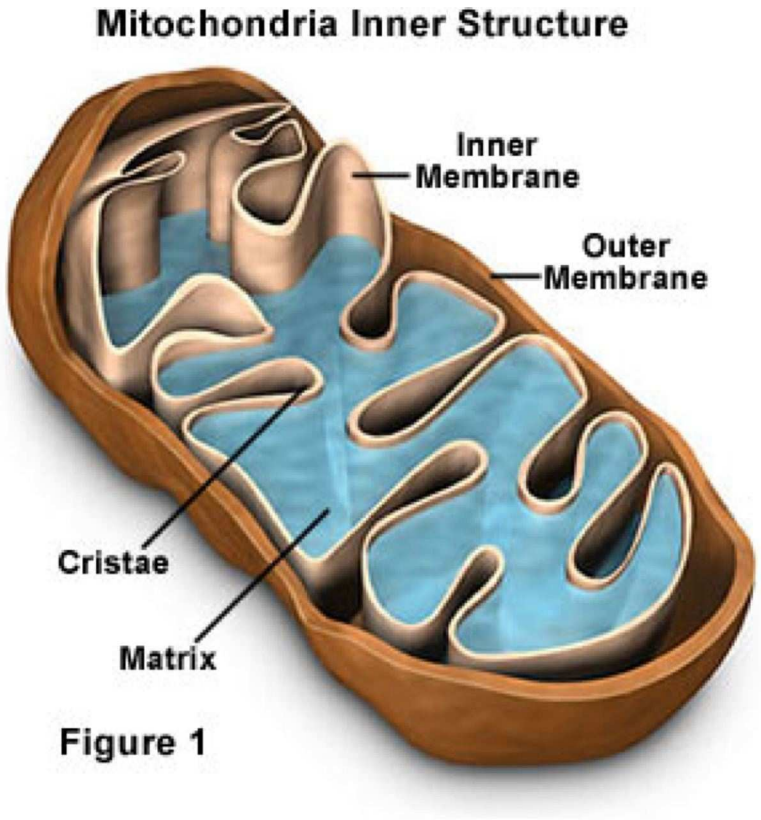

These organelles are the power generators of the cell, converting oxygen and nutrients into ATP (adenosine triphosphate). ATP is the chemical energy "currency" of the cell that powers the cell's metabolic activities. The mitochondrion is different from other organelles because it has its own DNA and reproduces independently of the cell in which it is found; an apparent case of endosymbiosis.

Fuel Cell Performance

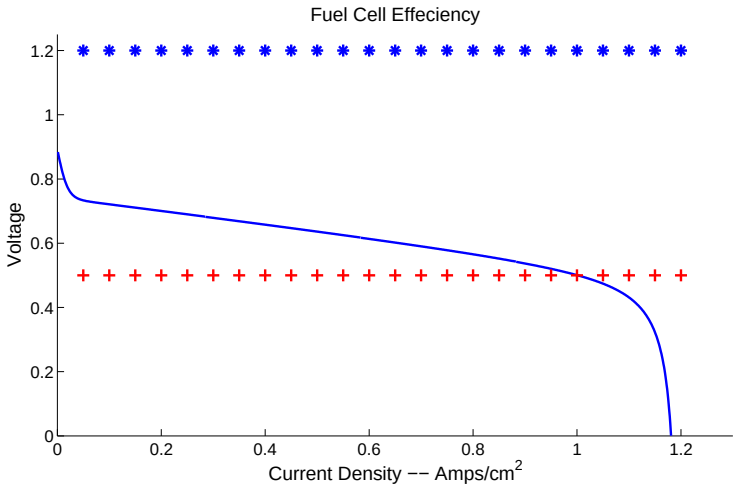

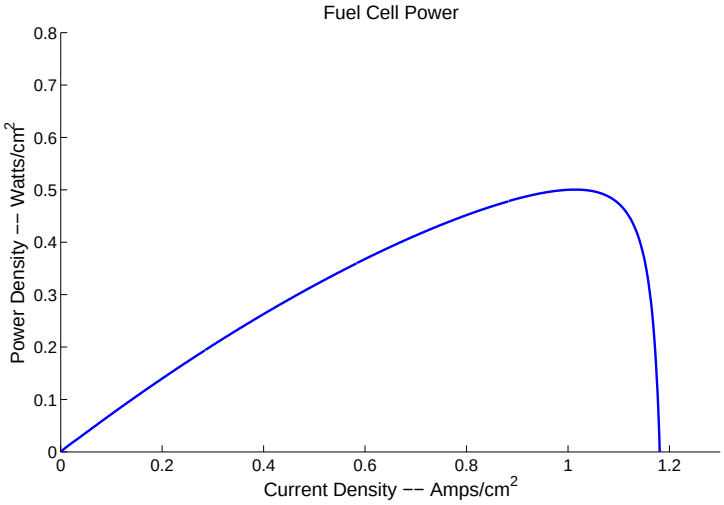

$$V = E_o - R * I - \eta(I, C_o)$$

Cell Voltage Balance

Power = $V * I$

Cell Power

Below the red line is the Cheetah regime

Fuel Cell Power: 0.5 Watts/cm^2 $\times$ **300** cm^2 = 150 Watts/cell

How do we get up to the kiloWatt regime? Answer Stacks.

Fuel Cell Stacks

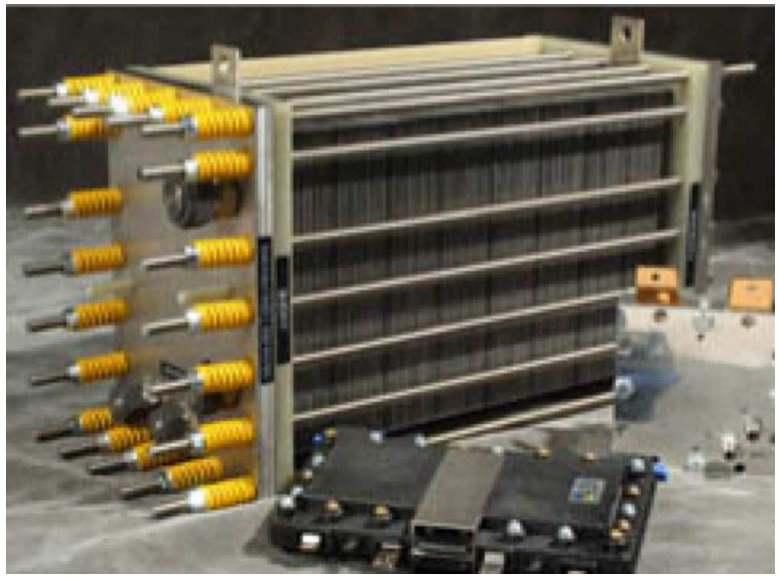

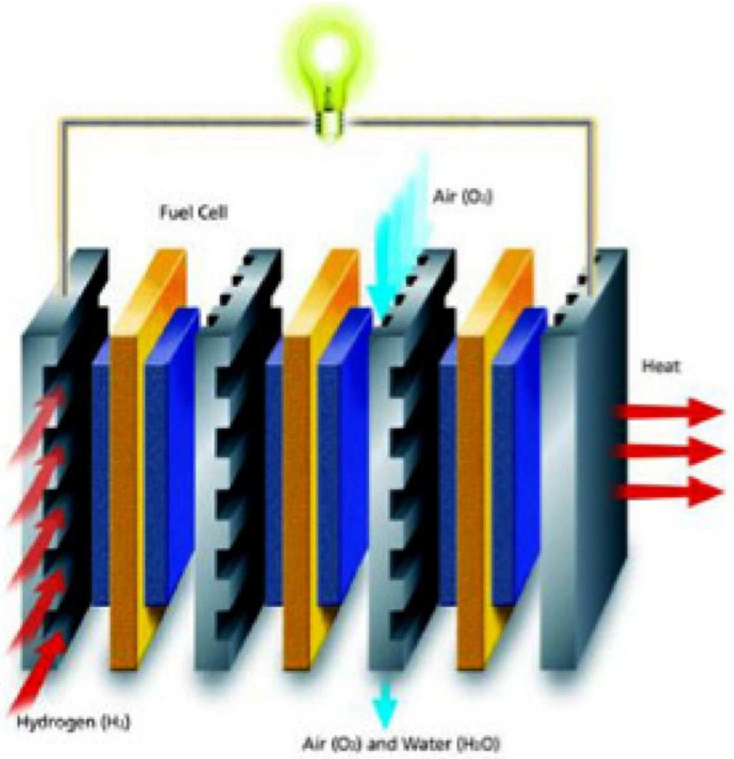

Fuel Cell Issues

Want to develop new (cheaper, higher temperature) polymer electrolyte membranes

Liquid water builds up in catalyst layers and clogs oxygen transport (Flooding)

Catalyst layers can degrade when run at high voltage, most due to understoich (Carbon Corrosion). Pt dissolution is also a long-term degradation worry.

Would like higher temperature operation to avoid the Cheetah effect and to use non-precious metal (cheaper) catalysts.

II) Scientific Overview: The Unit Cell

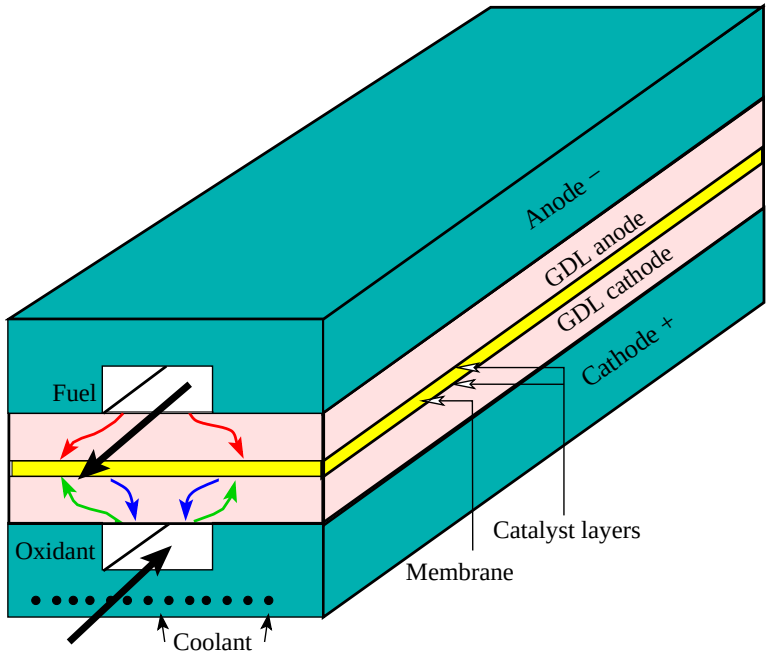

Channels: Variation of O_2, H_2, and H_2O from inlet to outlet.

GDL: Oxygen and vapor counter-diffusion, two-phase flow, formation of condensation/evaporation fronts.

Catalyst Layers: Production of H_2O and heat at cathode catalyst layers. Build-up of double-layer charge at catalyst interface.

Membrane: Ion and water motion in membrane, proton conduction, forms barrier for fuel, gases, e^-.

Coolant: Dominates cell temperature in long direction.

Presence of disparate length and time-scales for lengths $> 1\mu$ meter.
Functional structure at all length scales $< 1\mu$ meter.

Ionomer Membrane Properties

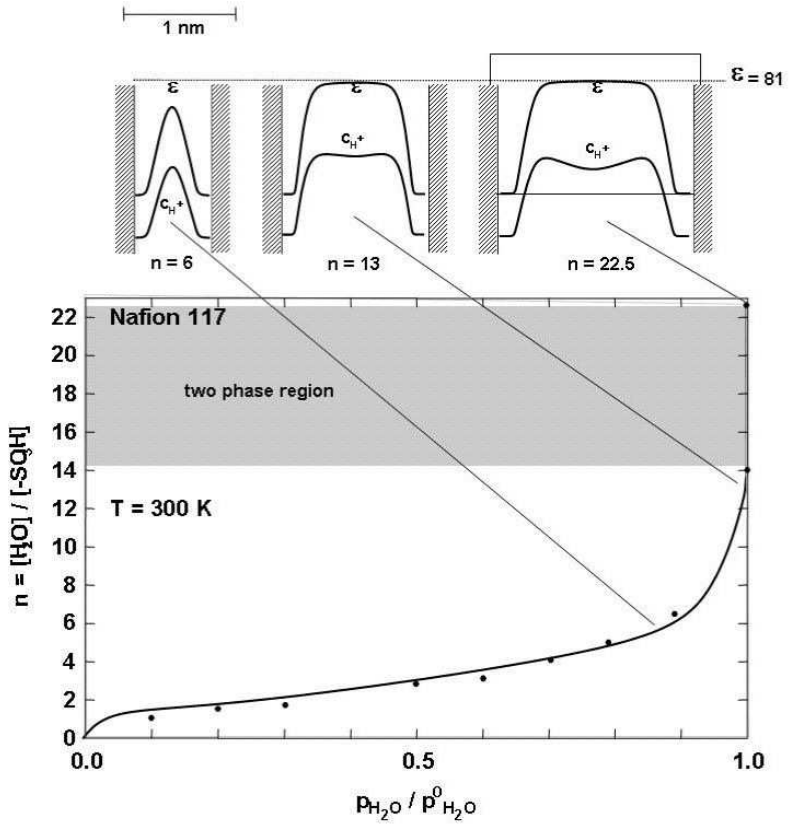

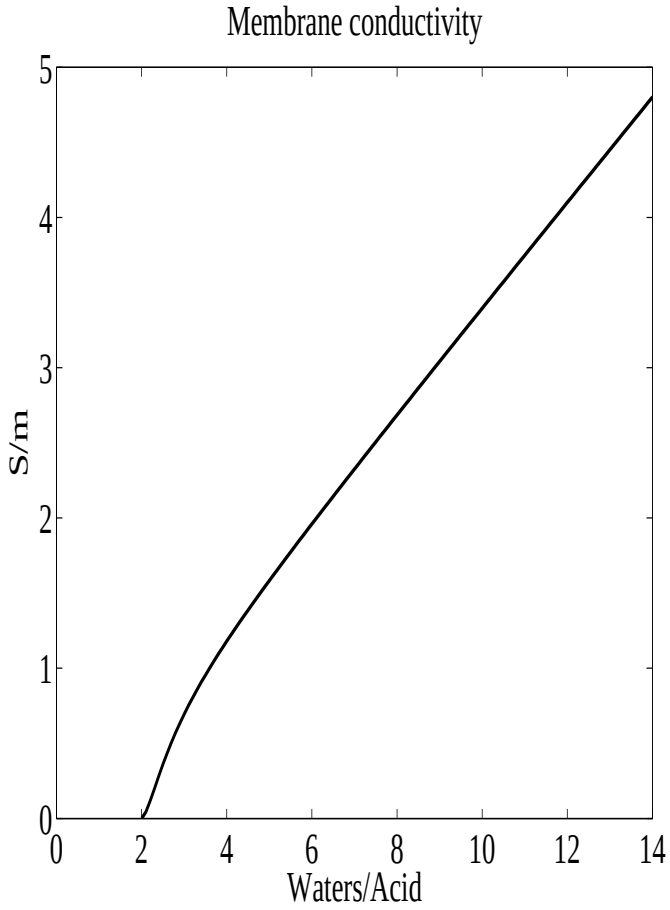

Nafion has three recognized forms, depending upon pretreatment (boiling in acid/desiccating):
Expanded (E), Normal (N), Shrunk (S).

(Left) The hydration isotherm for Normal form Nafion 117.
(Right) Protonic conductivity as a function of water content.

Catalyst Layer Properties

Figure 1

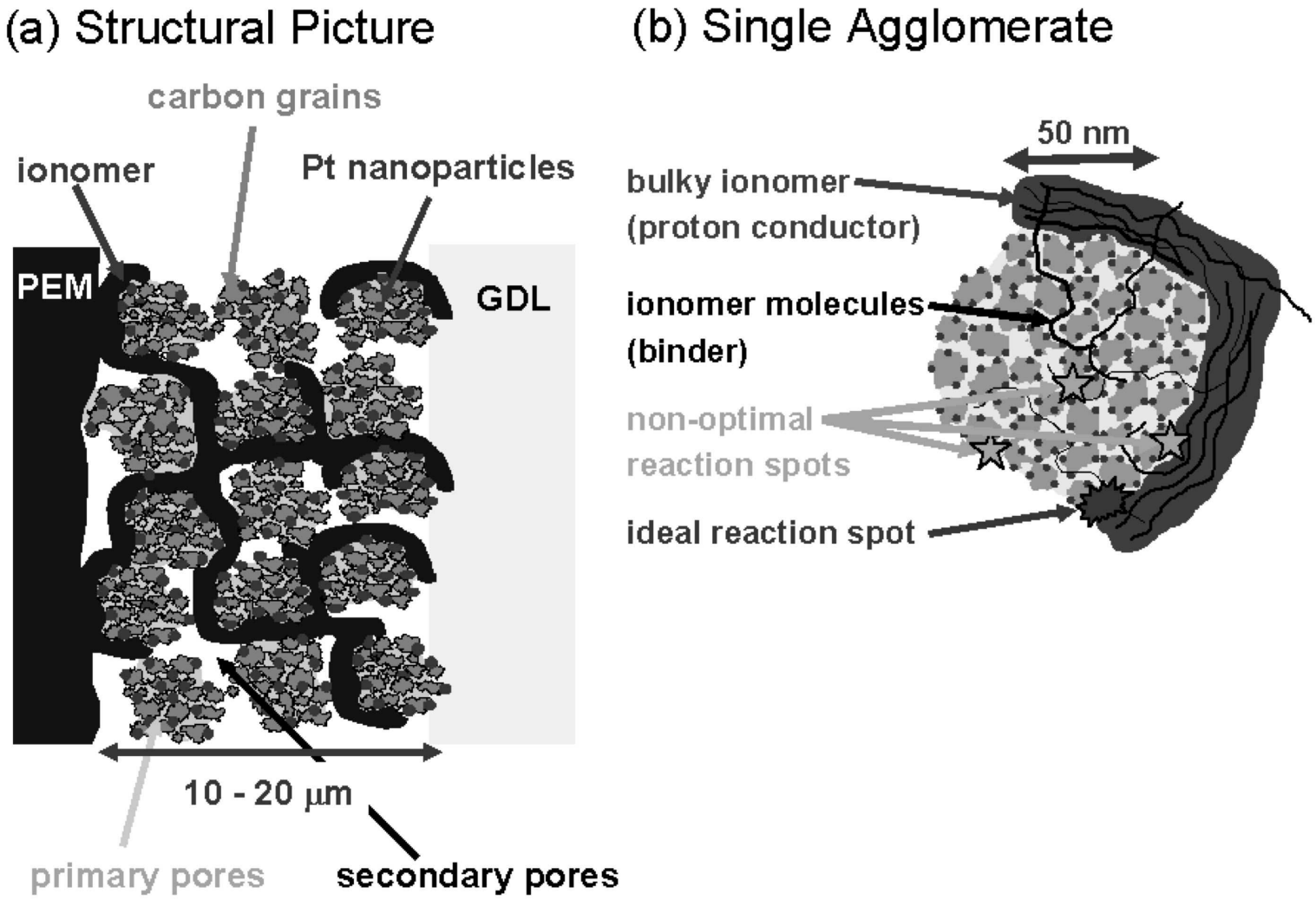

Cross-sectional Slice

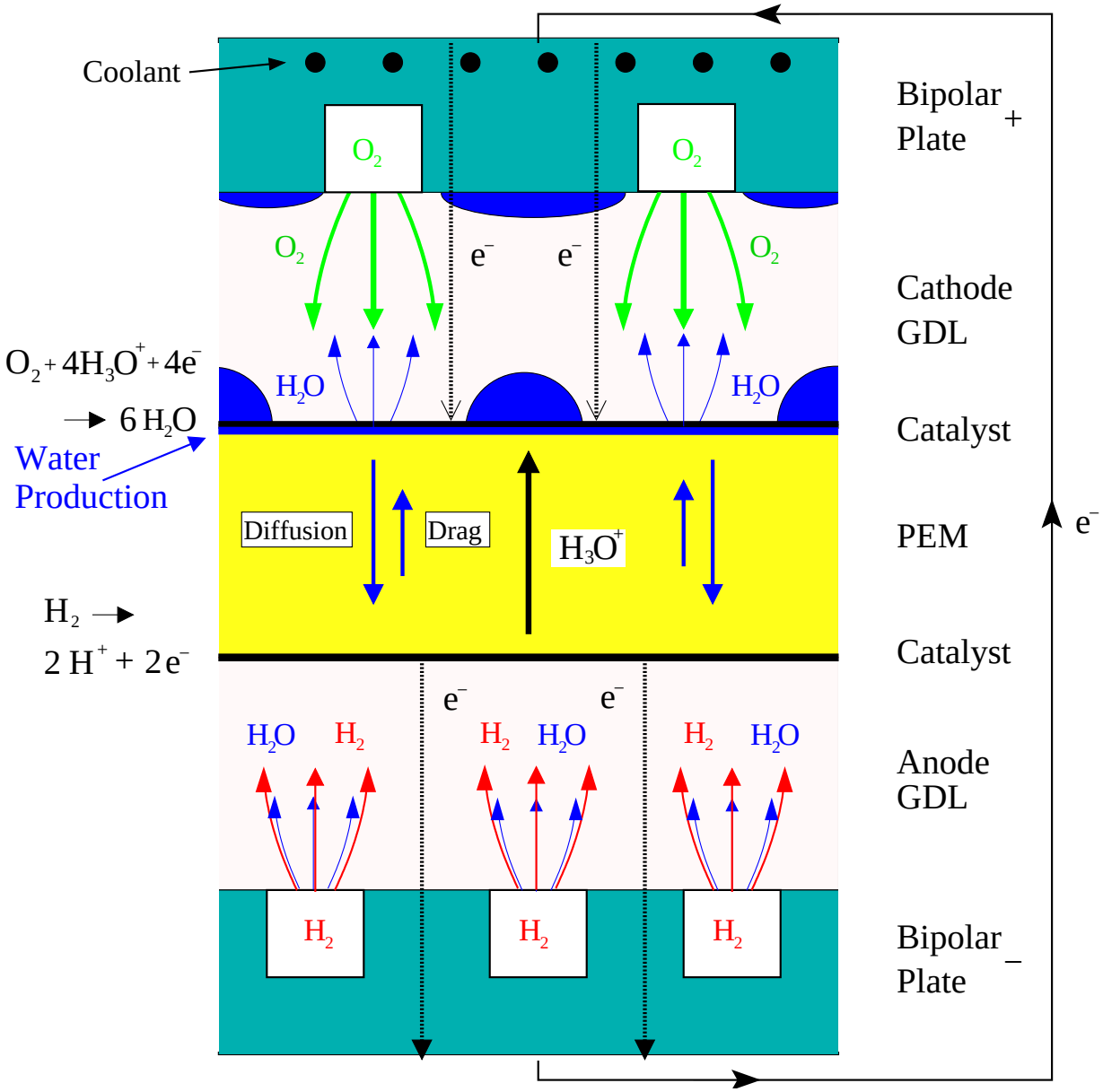

Transient Phase Change

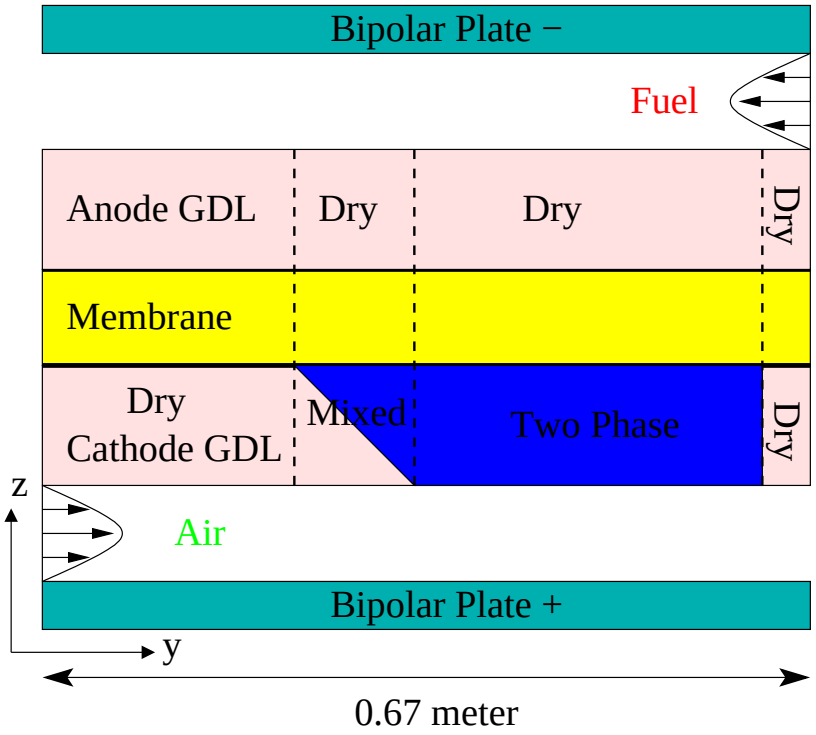

Break cell into Dry, Two-phase, and a Boundary Layer regime.
Exact solutions in Dry and Two-phase yield flux imbalance at wet-dry interface.
Leads to explicit ODE for slow front evolution.

K. P., J. Stockie, B. Wetton, *Proc. Roy. Soc. London: Series A* **462** (2006).
P. Chang, H. Haas, K. P., B. Wetton *J. Electrochem. Soc.* submitted.

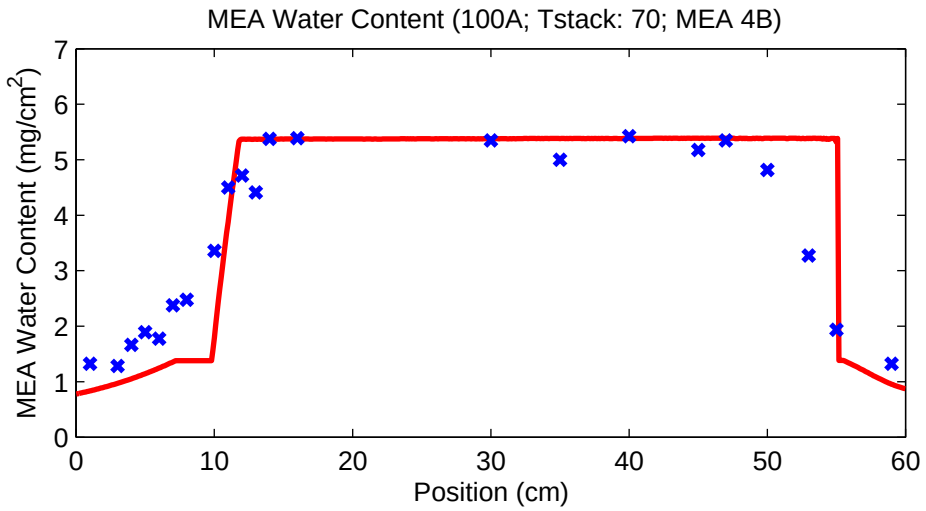

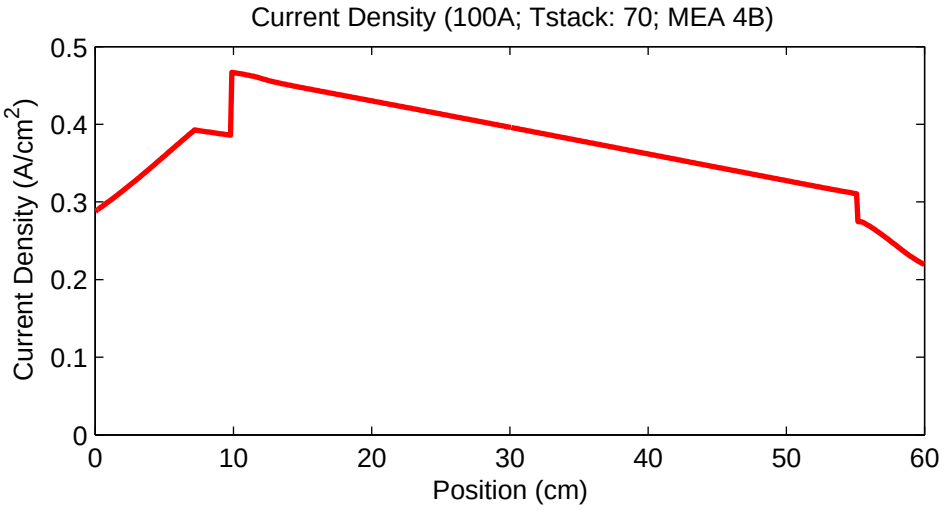

Operating Conditions

Fuel: H2
Fuel/Coolant: Counter
Fuel Inlet Pressure: 20.6 Psig
Fuel Dew Point: 57.2 C
Fuel Flow Per Cell: 1.12 SLPM

Ox: Air
Ox/Coolant: Co
Ox Inlet Pressure: 16.8 Psig
Ox Dew Point: 61.6 C
Ox Flow per Cell: 3.02 SLPM

Coolant Temp In: 68.9 C
Coolant Temp Out: 76.7 C
Load: 100 A

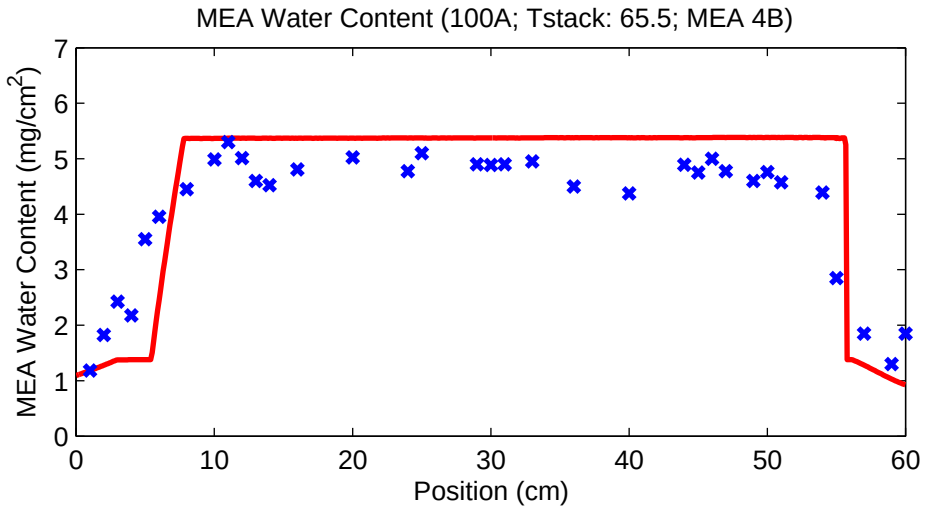

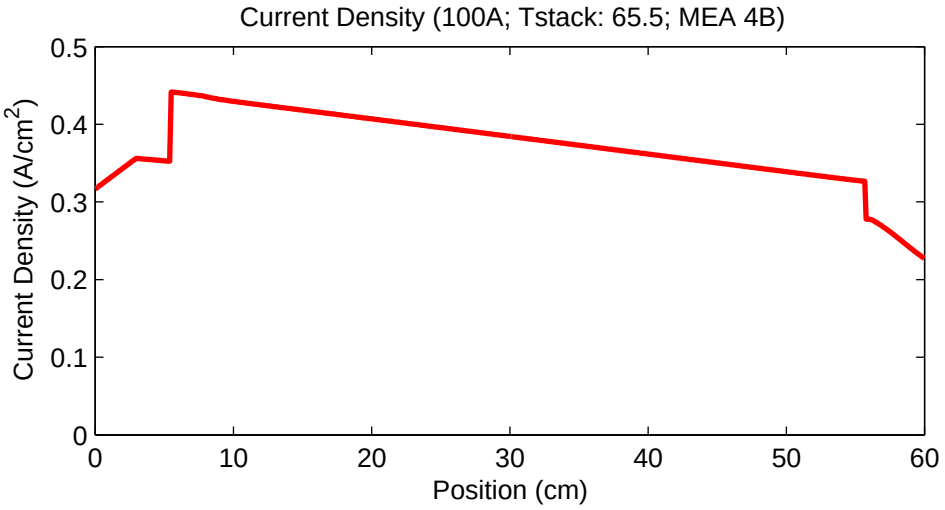

Operating Conditions

Fuel: H2
Fuel/Coolant: Counter
Fuel Inlet Pressure: 21.5 Psig
Fuel Dew Point: 57.7 C
Fuel Flow Per Cell: 1.4333 SLPM

Ox: Air
Ox/Coolant: Co
Ox Inlet Pressure: 18.2 Psig
Ox Dew Point: 61.8 C
Ox Flow per Cell: 3.88 SLPM

Coolant Temp In: 65.6 C
Coolant Temp Out: ? C
Load: 100 A

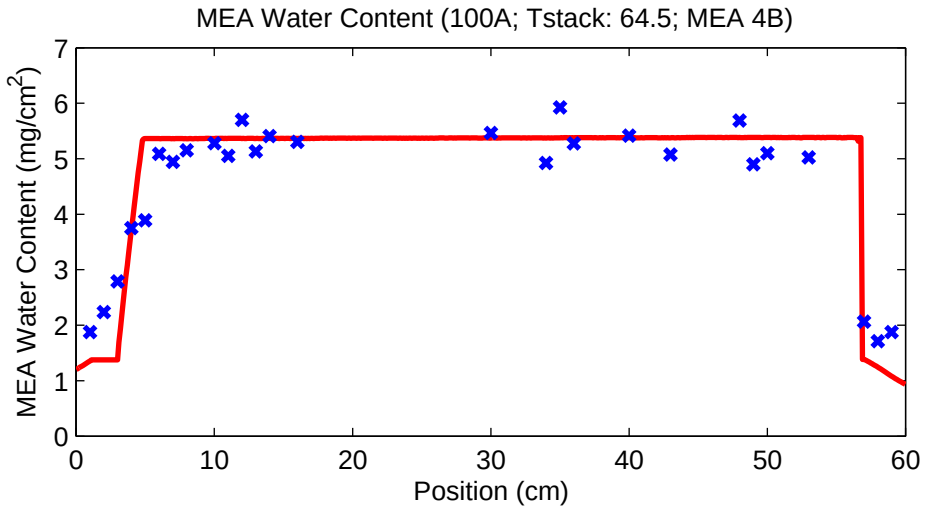

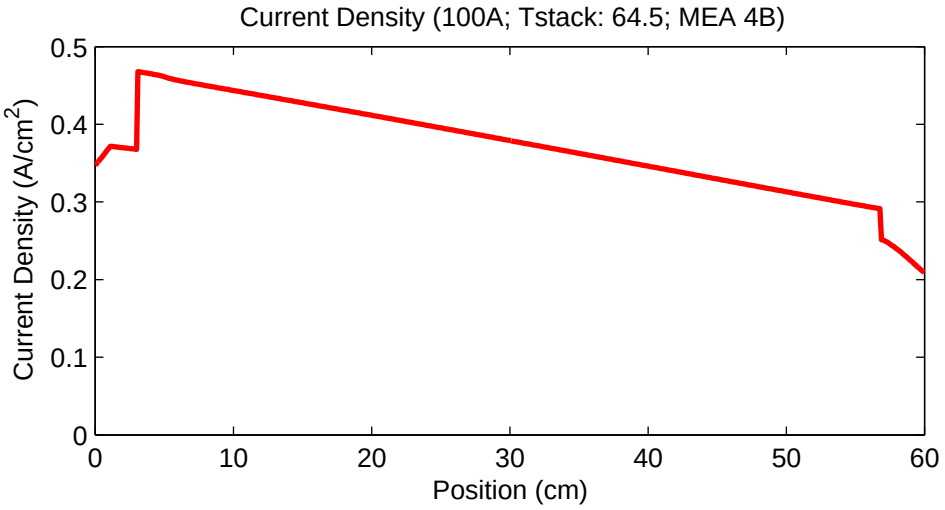

Operating Conditions

Fuel: H2
Fuel/Coolant: Counter
Fuel Inlet Pressure: 19.9 Psig
Fuel Dew Point: 57.6 C
Fuel Flow Per Cell: 1.0933 SLPM

Ox: Air
Ox/Coolant: Co
Ox Inlet Pressure: 16.7 Psig
Ox Dew Point: 61.5 C
Ox Flow per Cell: 2.94 SLPM

Coolant Temp In: 64.5 C
Coolant Temp Out: 70.1 C
Load: 100 A

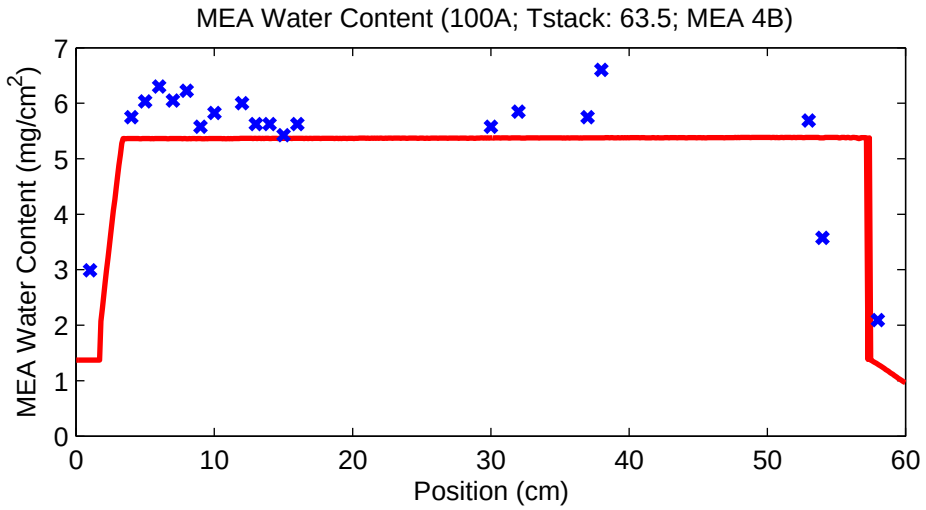

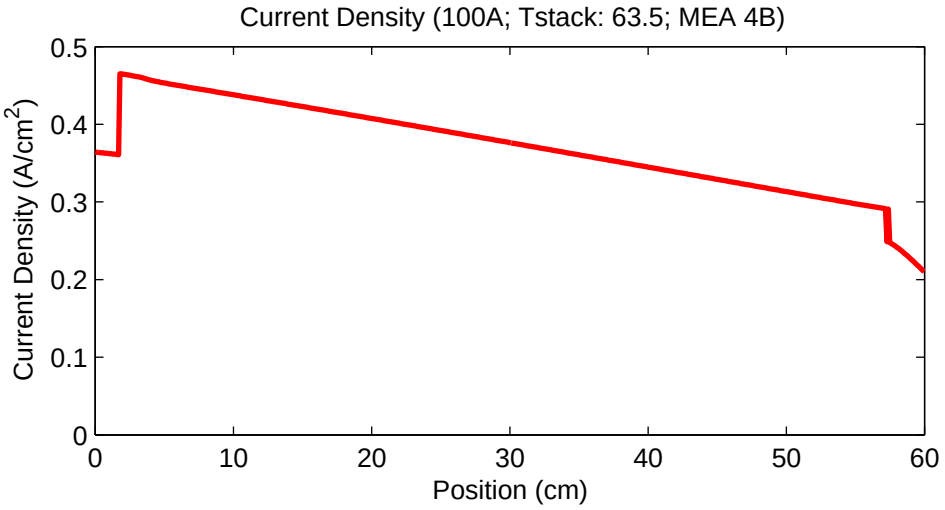

Operating Conditions

Fuel: H2
Fuel/Coolant: Counter
Fuel Inlet Pressure: 20.4 Psig
Fuel Dew Point: 57.7 C
Fuel Flow Per Cell: 1.1 SLPM

Ox: Air
Ox/Coolant: Co
Ox Inlet Pressure: 17.1 Psig
Ox Dew Point: 61.7 C
Ox Flow per Cell: 2.9933 SLPM

Coolant Temp In: 63.5 C
Coolant Temp Out: 69 C
Load: 100 A

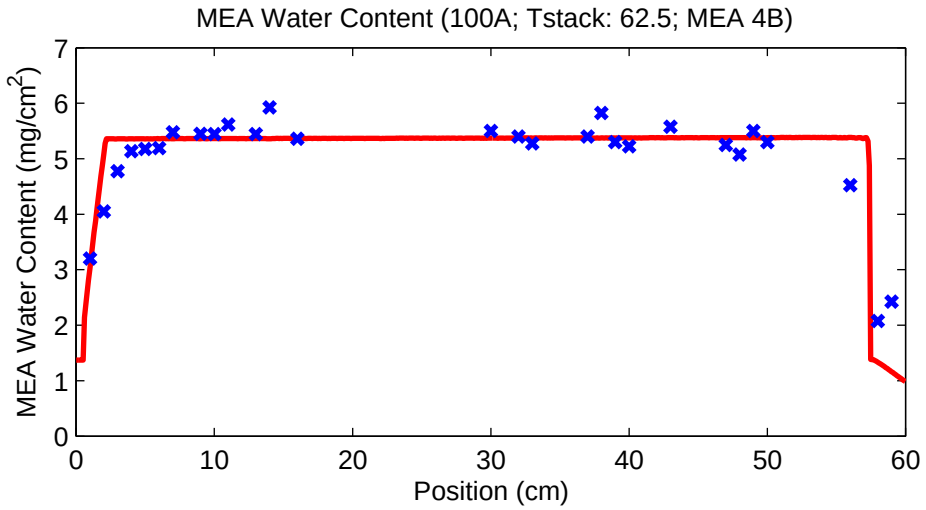

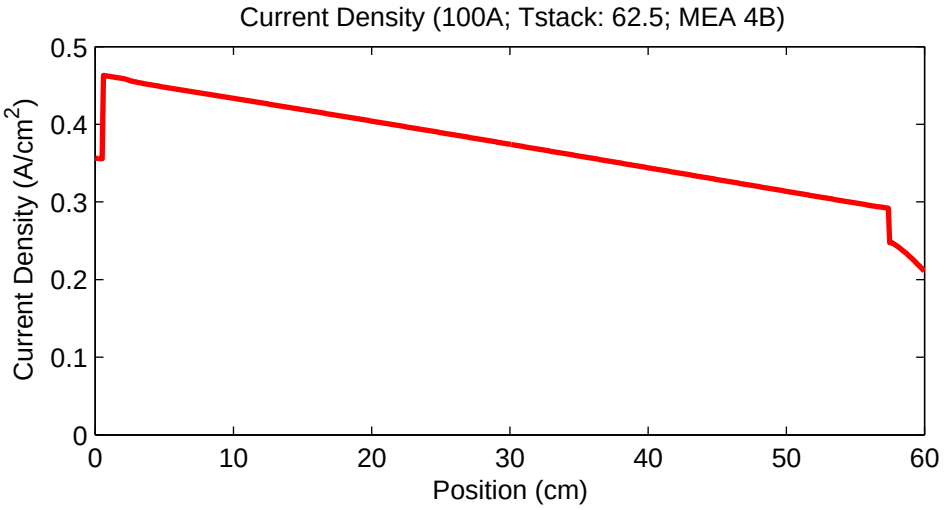

Operating Conditions

Fuel: H2
Fuel/Coolant: Counter
Fuel Inlet Pressure: 20.8 Psig
Fuel Dew Point: 57.5 C
Fuel Flow Per Cell: 1.1133 SLPM

Ox: Air
Ox/Coolant: Co
Ox Inlet Pressure: 16.9 Psig
Ox Dew Point: 61.7 C
Ox Flow per Cell: 3.0533 SLPM

Coolant Temp In: 62.6 C
Coolant Temp Out: ? C
Load: 100 A

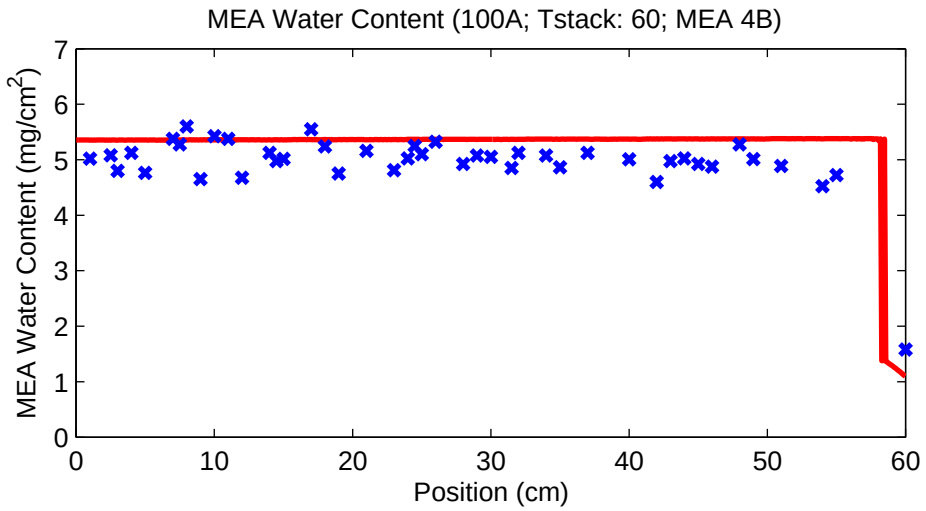

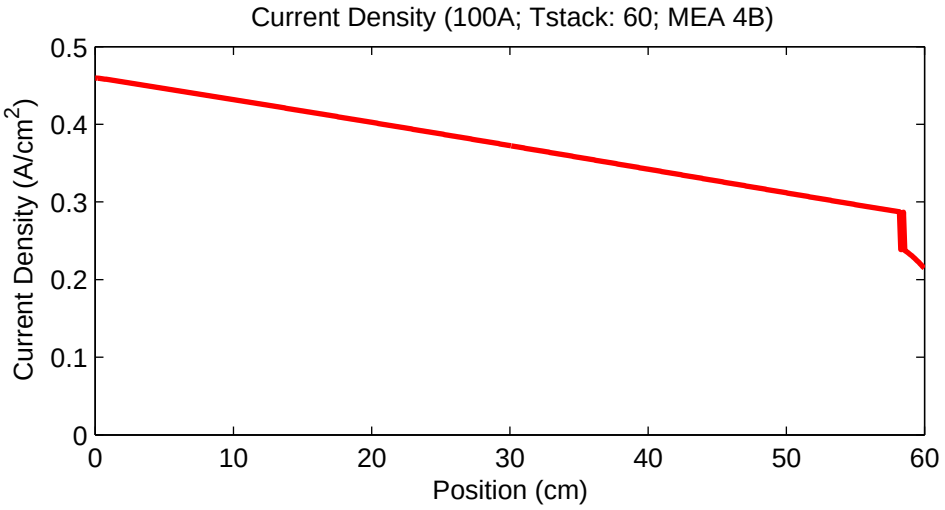

Operating Conditions

Fuel: H2
Fuel/Coolant: Counter
Fuel Inlet Pressure: 20.5 Psig
Fuel Dew Point: 57.5 C
Fuel Flow Per Cell: 1.12 SLPM

Ox: Air
Ox/Coolant: Co
Ox Inlet Pressure: 16.8 Psig
Ox Dew Point: 61.7 C
Ox Flow per Cell: 3.0133 SLPM

Coolant Temp In: 59.9 C
Coolant Temp Out: 67.4 C
Load: 100 A

Lateral Diffusion – Low Current Density

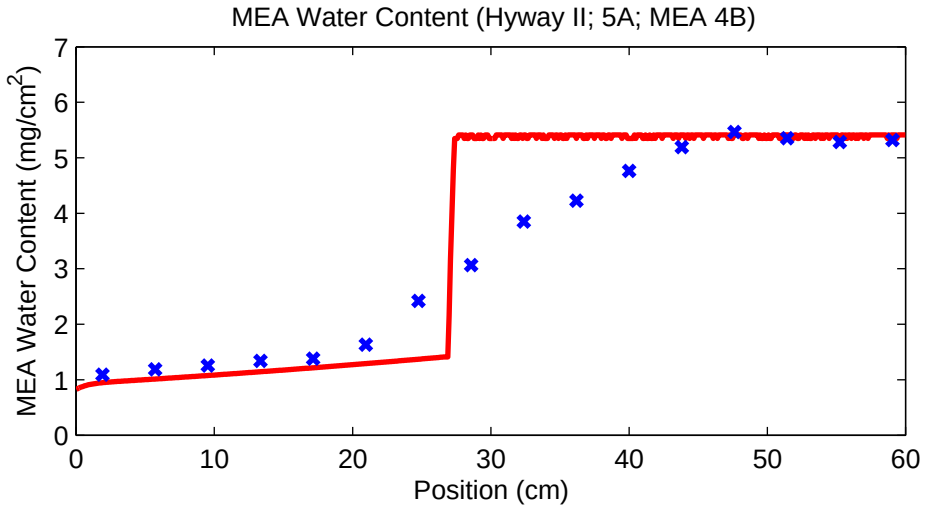

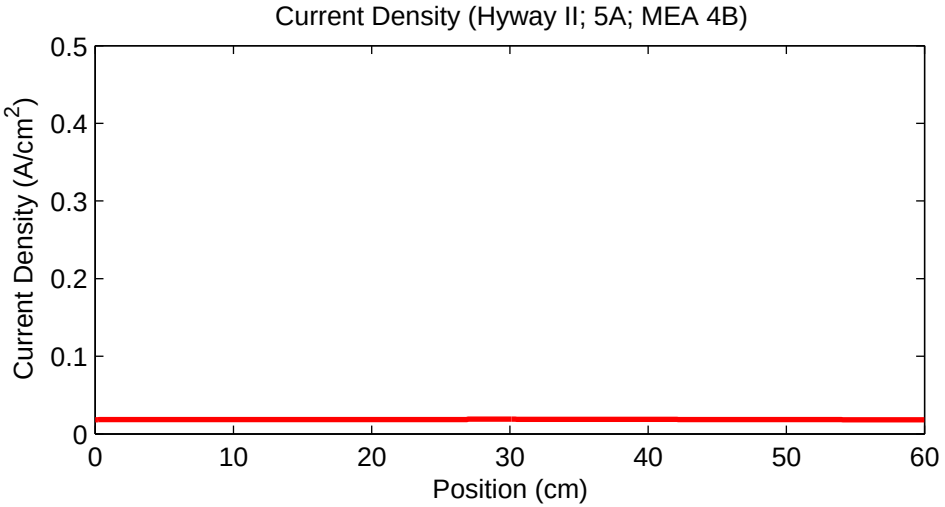

Operating Conditions

Fuel: H2:70% N2:30%
Fuel/Coolant: Co
Fuel Inlet Pressure: 20 Psig
Fuel Dew Point: 53 C
Fuel Flow Per Cell: 0.49 SLPM

Ox: Air
Ox/Coolant: Co
Ox Inlet Pressure: 16.7 Psig
Ox Dew Point: 59 C
Ox Flow per Cell: 0.9 SLPM

Coolant Temp In: 60 C
Coolant Temp Out: 61 C
Load: 5 A

III) Pore Formation in Polymer Electrolytes

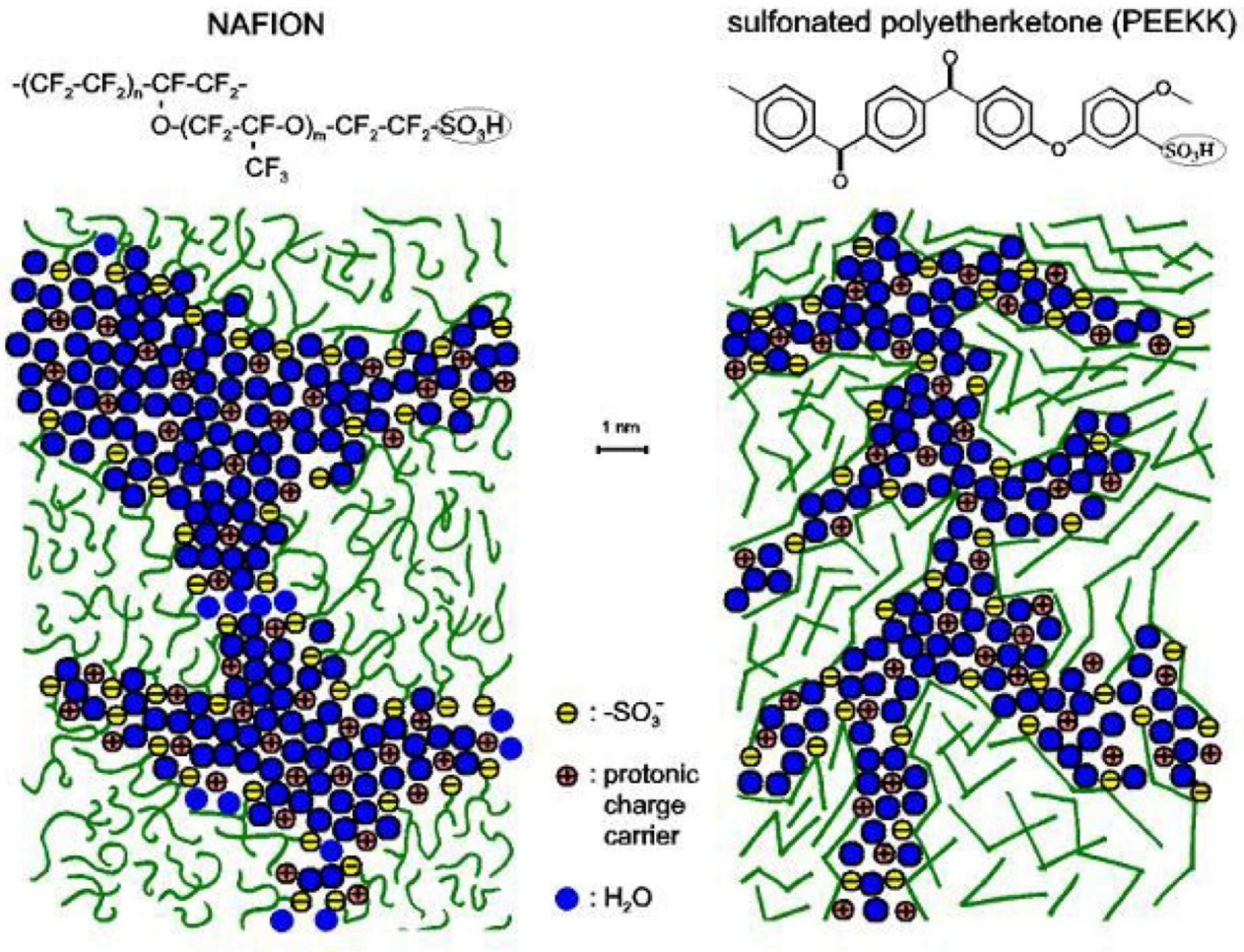

Nafion is hydrophobic, cross-linked polymer with hydrophilic (acidic) side-chains. Nafion phase-separates in presence of water forming a nano-scale liquid domain. Two-dimensional illustration of the channel nano-structural features of Nafion (left inset) and PEEKK (right inset) K.-D. Kreuer, *J. Memb. Sci.* **185** (2001) 29.

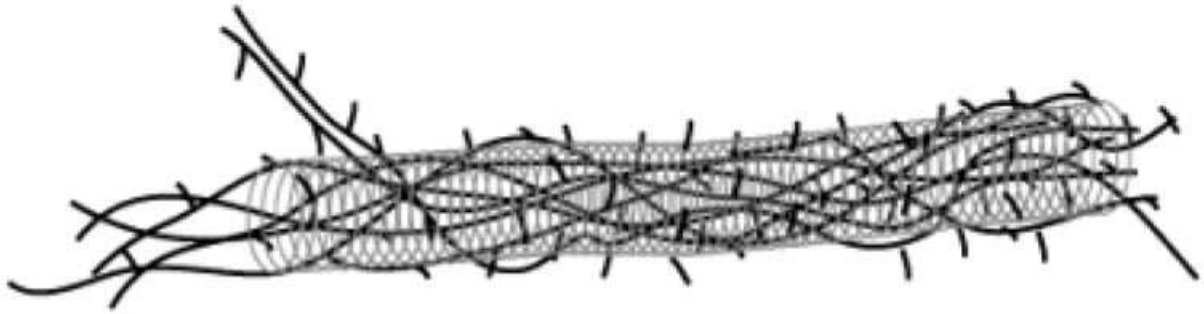

An interpretation, from Rubatat and Diat (2004), of the structure of Nafion channels based upon SAX and TEM scattering data.

Earlier work of Hsu and Gierke (1981) (1983) postulated that a balance of elastic deformation and hydrophilic surface interactions leads water to form spherical hydrophilic clusters of 4nm radius surrounded by sulfonate groups, with the clusters connected through cylindrical channels of 1nm diameter.

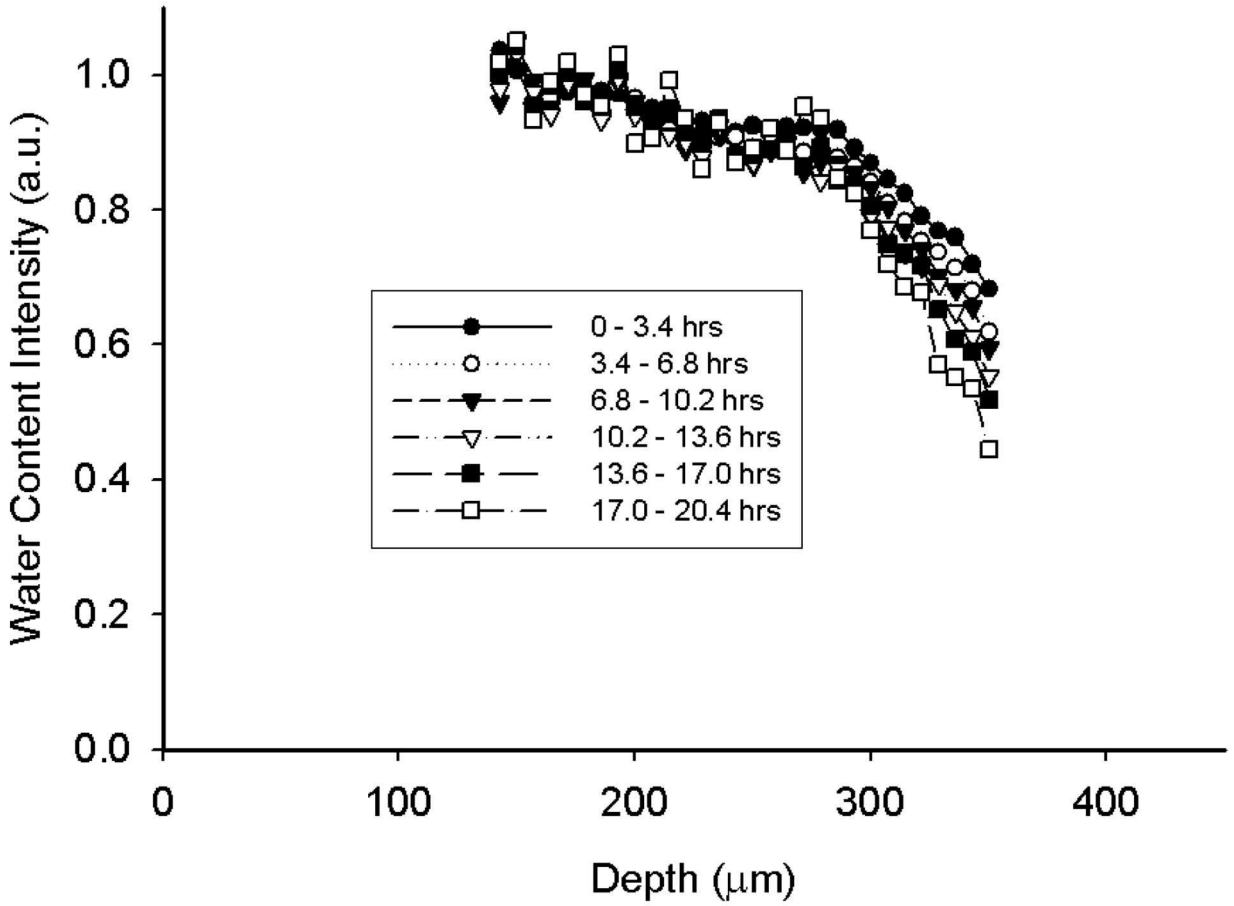

In-situ MRI data of Nafion membrane exposed on one side to liquid water and on the other air at constant RH, (Z. Zhang, B. Balcom, K. Promislow, et al submitted to JMR). The membrane is initially fully hydrated, but dries partially on the air side over a period of 24 hours. The time scale supports the idea of an internal rearrangement of pore structure.

Computational Approaches: Ab Initio

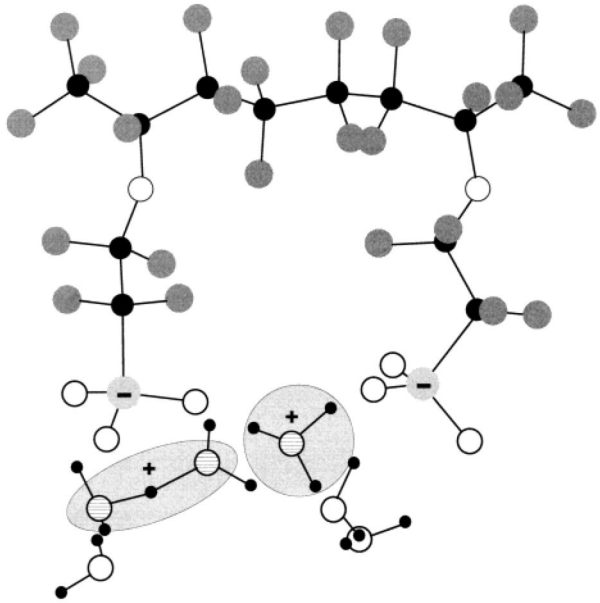

Ab-initio electronic structure theory starts from the Schrödinger equation for each relevant electron and nucleus. Computes chemical reactions on time scales from the Femtosecond ($\mathbf{10^{-15}}$) up to the Picosecond ($\mathbf{10^{-12}}$), and length scales on the order of Angstroms.

The figure shows the minimal energy conformation of a two-sidechain fragment of a perfluoro sulfonic acid polymer (Dow) with six water molecules, showing the dissociation of both acidic protons (Paddison, *S. J. Annu. Rev. Mater. Res.* 2003, **33**, 289).

Variation of Dielectric

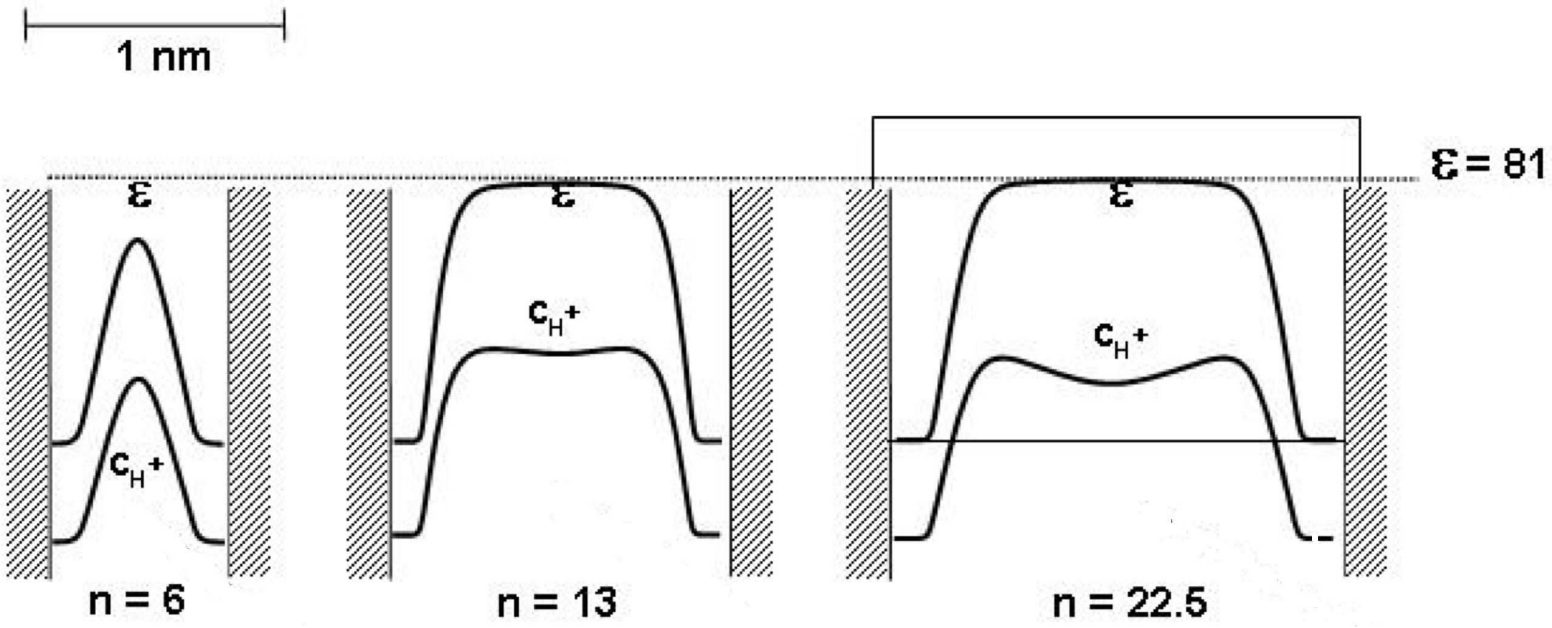

Profiles of the dielectric constant and protonic charge carrier concentration in a hydrated hydrophilic channel (pore) at three different water contents. Segregation of cationic and anionic charges leads to exceptional proton mobility.
K.-D. Kreuer, S. J. Paddison, *et. al.*, *Chem. Rev.* **104** (2004) 4637.

MD Simulations

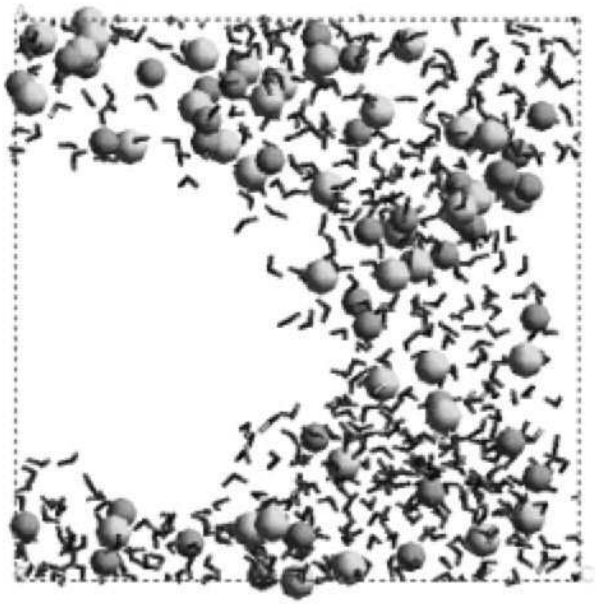

Small system

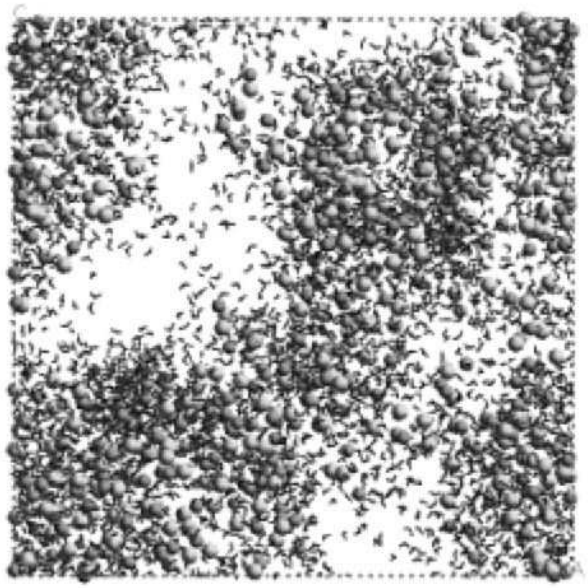

Big system

Molecular dynamics replaces electronic structure with partial charges, it can resolve time scales on the range of 100 picoseconds to nanoseconds ($\mathbf{10^{-6}}$) and length scales on the order of 10s of nanometers.
Figure shows phase segregated structure of hydrated Nafion. Nafion backbone has been deleted from the image, hence the white regions are crystalline Nafion (Jang, Molinero, Goddard, *J. Phys. Chem. B* **108** 2004).

Density Functional Theory

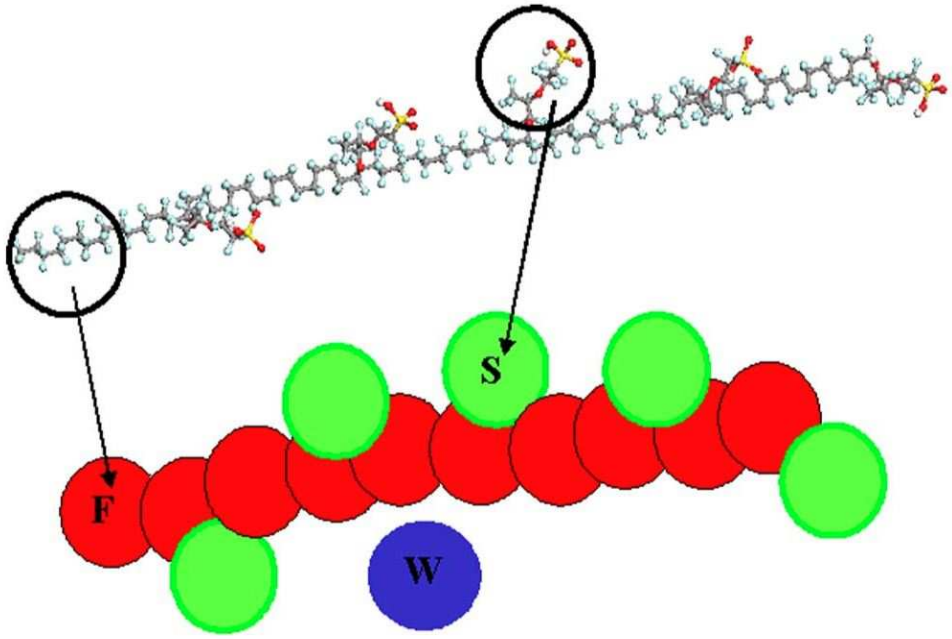

Density functional theory (DFT) is a course grained representation which places degrees of freedom into an effective Hamiltonian and uses statistical mechanics to calculate probable configurations (constrained minimizers of the Hamiltonian).

The figure depicts Nafion with its backbone broken into segments, the pendant acid groups become effective particles and water may be treated either implicitly or explicitly, (J. Wescott, Y. Qi, L. Subramanian, and T. Capehart, *Journal of Chemical Physics* **124** (2006)).

Phase Separation in DFT

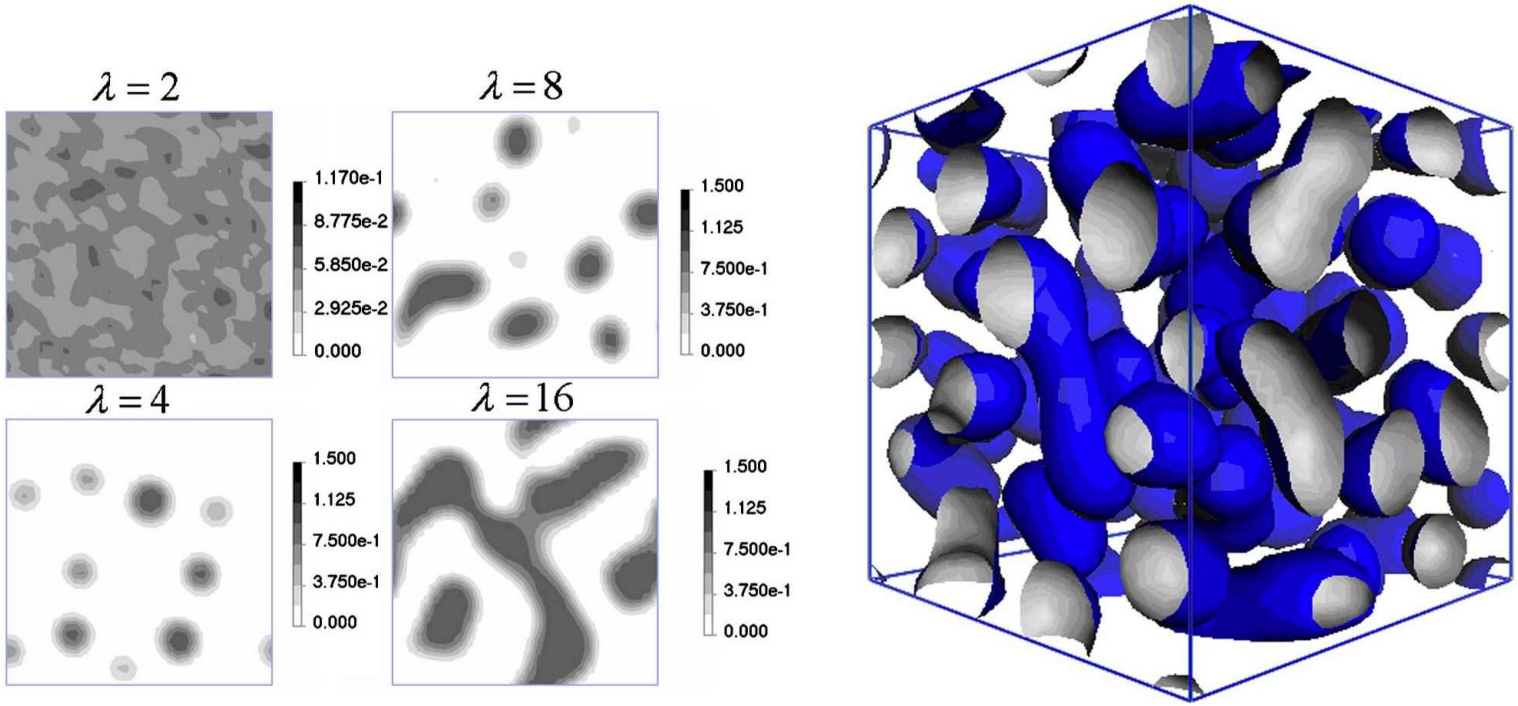

Phase separation of Nafion at various levels of hydration. Around 8 waters/acid group a pore structure starts to emerge. This approach computes steady state, can do linear response theory, but cannot compute hysteretic effects.

Conductive Polymer Electrolyte Equations

Model length scales of 1-1000 nanometers, upscaling nanostructure to macroscopic behavior, predict hysteresis and structural evolution on the order of minutes and hours. We want models that are amenable to analysis.

Introduce a phase-field function ψ, which takes the value 1, for the solvent domain, and -1, for the polymer domain.

Incorporate electrostatic, interfacial, and elastic energy densities in a momentum balance.

Pull the Lagrangian deformation of the elastic polymer back into Eulerian coordinates and solve a "seamless" PDE for fluid and elastic polymer.

Solve Poisson's equation and the Poisson-Nernst-Planck equation for the proton transport.

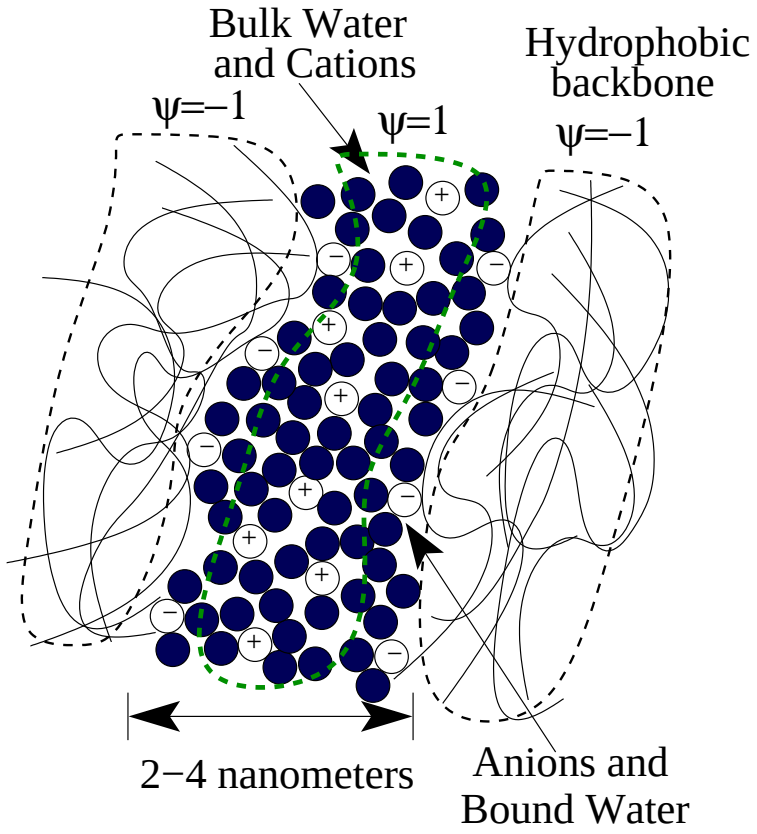

Phase Field Model

Incorporate ideas of
C. Liu and N. Walkington, *Arch. Rat. Mech. Anal.*, **159** (2001)
C. Liu and J. Shen, *Physica D* **179** (2003).

$x = x(X,t)$ Eulerian deformation in terms of Lagrangian X
$v = x_t$ Local velocity
$F = \frac{\partial x}{\partial X}$ Deformation gradient

Combine conservation of Mass and Momentum with Poisson-Nernst-Planck equations.

$$
\begin{aligned}
\psi_t + v.\nabla\psi &= \mathcal{G}\frac{\delta \mathcal{I}}{\delta \psi}, \\
p_t + v.\nabla p &= \nabla.\left(\mathcal{S}\nabla\left(\frac{p}{\mathcal{S}}\right) + p\nabla\phi\right), \\
v_t + v.\nabla v + \nabla\pi &= \nabla(\mu(\psi)\nabla v) + \nabla\cdot(\mathcal{D}\mathcal{W}F^t) + \frac{\delta\mathcal{E}}{\delta x} + \frac{\delta\mathcal{I}}{\delta x}, \\
\nabla.(\varepsilon\nabla\phi) &= n - p, \\
F_t + v.\nabla F &= (\nabla v)F, \\
\nabla.v &= 0, \\
\det F &= 1
\end{aligned}
$$

Electrostatic Energy and Charge Distribution

Denoting by $d = d(x)$ the signed distance to the $\psi = 0$ interface the relative permittivity varies rapidly in d, $\varepsilon = \varepsilon(x) = \varepsilon(d(x)/\epsilon)$, where the length scale $\epsilon \ll 1$.

The (scaled) electrostatic energy density is given in terms of the electric potential ϕ and ε,

$$\mathcal{E}(\phi, \psi) = \frac{1}{2} \int_{\Omega} \varepsilon |\nabla \phi|^2 dx.$$

The electrostatic energy density gradient

$$\frac{\delta \mathcal{E}}{\delta x} = \frac{\delta \mathcal{E}}{\delta \phi} \nabla \phi + \frac{\delta \mathcal{E}}{\delta \varepsilon} \nabla \varepsilon = (p - n) \nabla \phi + \frac{1}{2} |\nabla \phi|^2 \nabla \varepsilon.$$

The negative charges are tethered and localized near the interface, we take their density to be prescribed: $n = n(d/\epsilon)$. The hydrogen bond network upon which the protons walk is depleted in the low-permeativity regions. Denoting the local density of the hydrogen bond network by $\mathcal{S} = \mathcal{S}(\varepsilon)$, it is the proton entropy $p/\mathcal{S}$ which effectively diffuses, resulting in an apparent "entropic force"

$$p_t + v . \nabla p = \nabla . \left(\nabla p + p \nabla \phi - \overbrace{p \nabla \ln \mathcal{S}}^{Entropic\ Force} \right).$$

Interfacial Energy Density

In functionalized polymers the polymer-solvent interfacial energy dominates at 1-5 nanometer length-scales

$$\mathcal{I}(\psi) = \mathcal{H}(\psi) - \eta \mathcal{A}(\psi)$$

where η is the ratio of energy density associated to the acid groups to the energy density of the bending moments. Boiling means large η, drying/cooling means small η.

Square of mean curvature

$$\mathcal{H} = \frac{1}{2} \int_\Omega \left(\epsilon \Delta \psi - \frac{1}{\epsilon} f(\psi) \right)^2 \, dx$$

Surface area

$$\mathcal{A} = \int_\Omega \left(\frac{\epsilon}{2} |\nabla \psi|^2 + \frac{1}{\epsilon} F(\psi) \right) \, dx$$

where $F(s) = \frac{1}{4}(s^2 - 1)^2$ is the double well and $f(s) = F'(s) = (s^2 - 1)s$. The length scale ϵ controls the thickness of the polymer-solvent transition region.

Under a monotonicity assumption on $\partial_x^2 \psi$ it is known that $\epsilon^{-1}\mathcal{H}$ converges to the Willmore functional as $\epsilon \to 0$ (R. Moser 2005 *SIAM Math. Anal.*). The Γ-limit of $\mathcal{A}$ is an area functional (L. Modica and S. Mortola 1977/ S. Mordica 1987/ P. Sternberg 1988/...).

Functionalized Polymer Electrolyte equations

Given a general Lagrangian density $\boldsymbol{L} = \boldsymbol{L}(\boldsymbol{\nabla}\boldsymbol{\psi}, \boldsymbol{\psi}, \boldsymbol{x})$, and associated Lagrangian

$$\boldsymbol{\mathcal{E}} = \int_{\Omega} \boldsymbol{L} d\boldsymbol{x},$$

we define the functionalized Lagrangian

$$\boldsymbol{\mathcal{F}}(\boldsymbol{\psi}) = \frac{\mathbf{1}}{\mathbf{2}} \int_{\Omega} \left(\frac{\boldsymbol{\delta}\boldsymbol{\mathcal{E}}}{\boldsymbol{\delta}\boldsymbol{\psi}} \right)^{\mathbf{2}} d\boldsymbol{x} - \boldsymbol{\eta}\boldsymbol{\mathcal{E}}(\boldsymbol{\psi}).$$

Functionalization

Take the dominant feature of a Lagrangian, flip its sign, and regularize with the square of the variational derivative.

The variational derivative factors,

$$\frac{\boldsymbol{\delta}\boldsymbol{\mathcal{F}}}{\boldsymbol{\delta}\boldsymbol{\psi}} = \frac{\boldsymbol{\delta}^{\mathbf{2}}\boldsymbol{\mathcal{E}}}{\boldsymbol{\delta}\boldsymbol{\psi}^{\mathbf{2}}} \frac{\boldsymbol{\delta}\boldsymbol{\mathcal{E}}}{\boldsymbol{\delta}\boldsymbol{\psi}} - \boldsymbol{\eta} \frac{\boldsymbol{\delta}\boldsymbol{\mathcal{E}}}{\boldsymbol{\delta}\boldsymbol{\psi}} = \left(\frac{\boldsymbol{\delta}^{\mathbf{2}}\boldsymbol{\mathcal{E}}}{\boldsymbol{\delta}\boldsymbol{\psi}^{\mathbf{2}}} - \boldsymbol{\eta} \right) \frac{\boldsymbol{\delta}\boldsymbol{\mathcal{E}}}{\boldsymbol{\delta}\boldsymbol{\psi}}.$$

The interfacial energy for the functionalized polymer/solvent mixture is the functionalization of surface area $\boldsymbol{\mathcal{A}}$.

$$\frac{\boldsymbol{\delta}\boldsymbol{\mathcal{I}}}{\boldsymbol{\delta}\boldsymbol{\psi}} = \boldsymbol{\epsilon}^{-\mathbf{2}} \left(\boldsymbol{\epsilon}^{\mathbf{2}}\boldsymbol{\Delta} - \boldsymbol{f}'(\boldsymbol{\psi}) + \boldsymbol{\epsilon}\boldsymbol{\eta} \right) \left(\boldsymbol{\epsilon}^{\mathbf{2}}\boldsymbol{\Delta} - \boldsymbol{f}(\boldsymbol{\psi}) \right).$$

FPE Gradient Flows

Uncouple the interfacial energy from remainder of the problem. Consider a fast time ($T = t/\epsilon^2$) gradient flow either in L^2 (Allen-Cahn like - mass not conserved)

$$U_T = -\epsilon^2 \frac{\delta \mathcal{I}(U)}{\delta U},$$

or a family of conservation laws (Cahn-Hilliard like)

$$U_T = \epsilon^2 \mathcal{G}_\rho \frac{\delta \mathcal{I}(U)}{\delta U},$$

where $\mathcal{G}_\rho = (1+\rho)\frac{\Delta}{I - \rho\Delta}$ interpolates between the Laplacian, $\mathcal{G}_0 = \Delta$ for $\rho = 0$, and the zero-mass projection $\mathcal{G}_\infty f = f - < f >$, as $\rho \to \infty$.

Movies – $\mathcal{G}_1$ Gradient Flows

Movie 1	Hot Roll-up from a flat Interface	$\eta = 1$	$\epsilon = 0.05$
Movie 2	Cold Roll-up from a developed interface	$\eta = 4\epsilon$	$\epsilon = 0.02$
Movie 3	Hot Roll-up from a circular solvent inclusion	$\eta = 1$	$\epsilon = 0.05$
Movie 4	Glassy state roll-up from flat interface	$\eta = 5$	$\epsilon = 0.02$
Movie 5	Coarsening from a glassey state	$\eta = 2\epsilon$	$\epsilon = 0.01$

Qualitative Comparison to Data

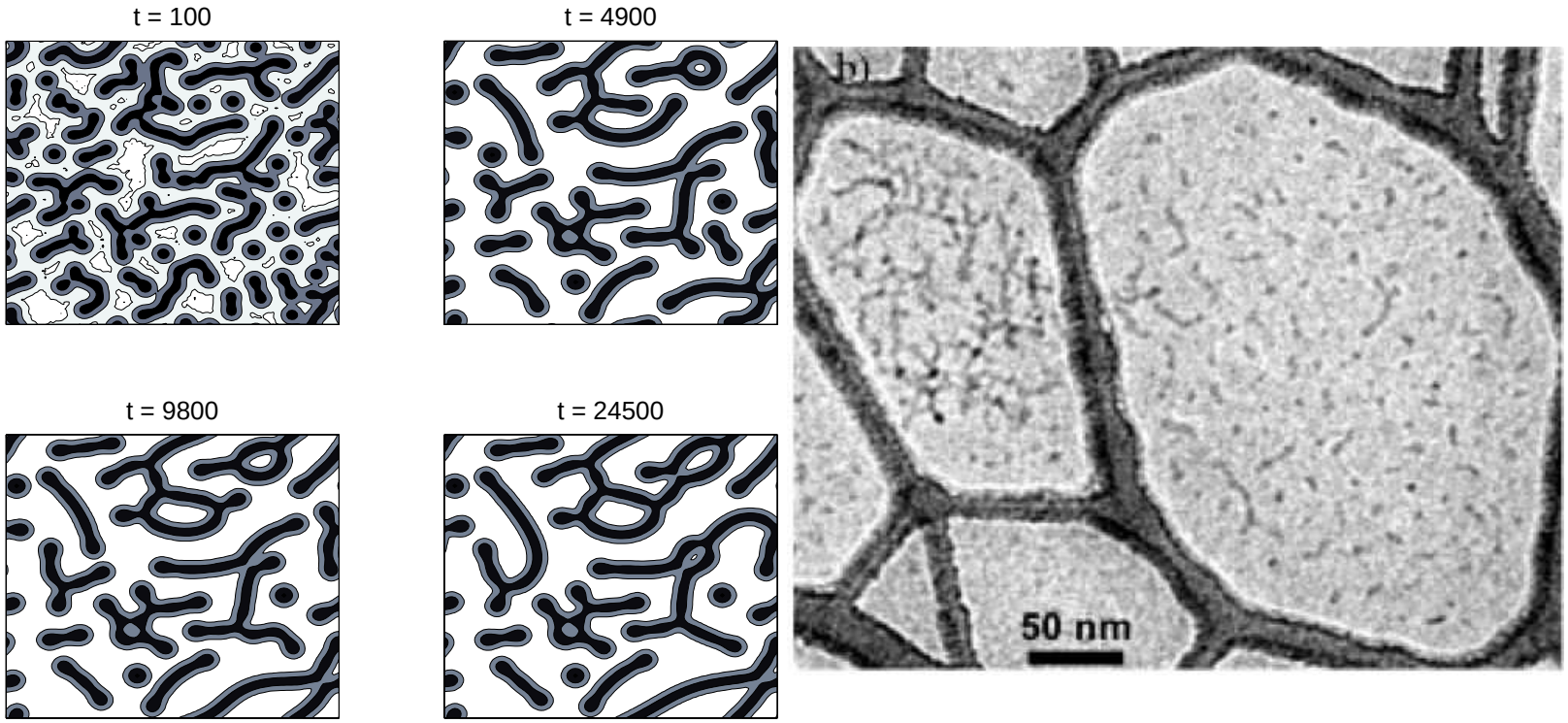

(Left) A 2D simulation of the $\mathcal{G}_1$ FPE gradient flow with periodic boundary conditions for an 80% Polymer (white) 20% solvent (dark) mixture starting from "well-boiled" initial data, with zero mean white noise added at each time step. Parameters are $\epsilon = 1.6 \times 10^{-3}$, $\eta = 2\epsilon$. (Right) Cryo-TEM image of Nafion 1100 solution from Rubatat and Diat (2004), who describe the solvent phase as "a network of wormlike structures." The lateral width of the image is roughly 100 nanometers. Dark spots are water, brighter is crystallized Nafion. The thick black lines are carbon inclusions which support the membrane.

MRI Data

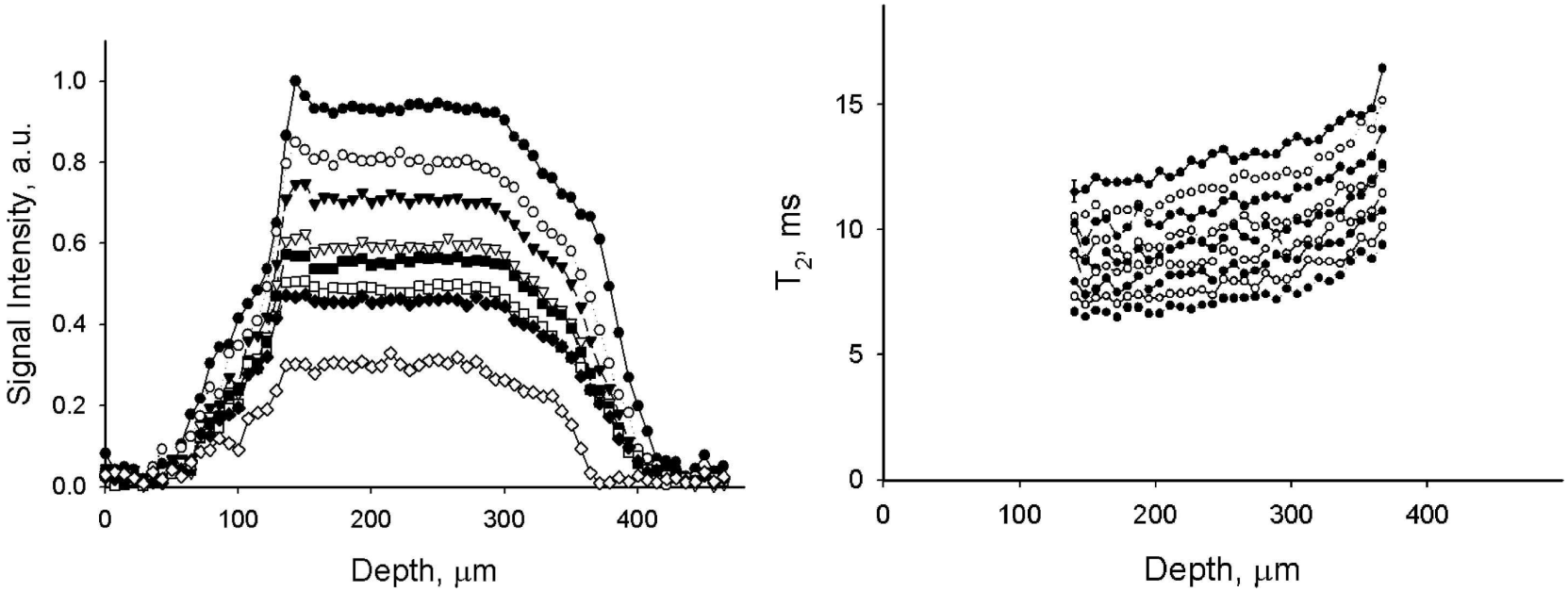

(Left) The full MRI signal intensity, which includes both factors from water content and signal lifetime (T2). The sample is liquid water equilibrated on the left and dried on the right. There is a clear dichotomy between water profiles with a break in slope towards the dry end. (Rigth) The averaged T2 signal which is associated with with percentage of water which are free/bound. There is a higher T2 value towards the dry end indicating a *greater* precentage of water in a bulk state, as compared to the dry end. Moreover the T2 value deceases sharply with time (aging effect) since the sample was initially prepared by boiling. The ageing effect is consistent with "defingering" as the sample coarsens from its boiled state.

Equilibrium Charge Density

The electrostatic, Nernst-Planck, and momentum balance equations are much faster to equilibrate than the interfacial energy. Take the phase separation ψ as given. Under zero flux conditions the proton density p and electric potential ϕ are determined by elliptic system

$$\begin{aligned} \nabla \cdot (\varepsilon(\psi)\nabla\phi) &= n(\psi) - p, \\ \nabla \cdot I &= 0, \end{aligned}$$

where the protonic current I takes the form

$$I = \nabla p + p\nabla\phi - p\nabla \ln \mathcal{S} = p\nabla\left(\phi + \ln\frac{p}{\mathcal{S}}\right).$$

In the absence of a driving force, such as an externally imposed electric field, not only is the divergence of the current zero, but the current itself is zero. The charge distribution becomes a function of the electric field,

$$p = p_0 \mathcal{S} e^{-\phi},$$

and Poisson's equation becomes a modified Poisson-Boltzmann equation

$$\nabla \cdot (\varepsilon(\psi)\nabla\phi) = n(\psi) - p_0 \mathcal{S}(\psi) e^{-\phi}.$$

The solvability of the modified Poisson-Boltzmann equation is equivalent to global electroneutrality, $< n >=< p >$, which determines the constant p_0.

Importance of Junction Shapes

Over the micron scale domain Ω, the effective conductivity tensor $\overline{\sigma}$ relates the averaged current density to the averaged potential gradient, $< I >= \overline{\sigma} < \nabla\phi >$. With a the charge density given from the electic potential $p = p(\psi)$ the potential is written as a static and a dynamic part, $\phi = \phi_0 + \phi_d$. The current is then given by the linear remnant of the Nernst-Planck equations

$$I = p(\psi)\nabla\phi_d.$$

The effective conductivity has the variational formulation

$$\sum_{i,j=1}^{3} \overline{\sigma}_{ij}\xi_i\xi_j = \min_{<\nabla\phi_d>=\xi} \langle p(\psi)\nabla\phi_d \cdot \nabla\phi_d \rangle ,$$

where ξ is an arbitrary vector in $\mathbf{R}^3$.

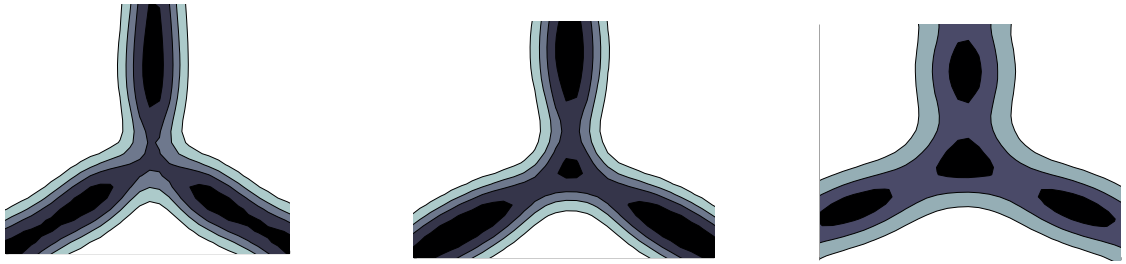

Pinch points at a three-channel junction for (left) $\epsilon = .01, \eta = 2$ with a single saddle point at the center of the juncture, (center) $\epsilon = .01, \eta = 2\epsilon$, with three saddle points, one on each arm of the junction, and (right) $\epsilon = .03, \eta = 1$, for which the channels are significantly wider.

IV) Nanophase Models: Macrohomogenious Catalyst Layer

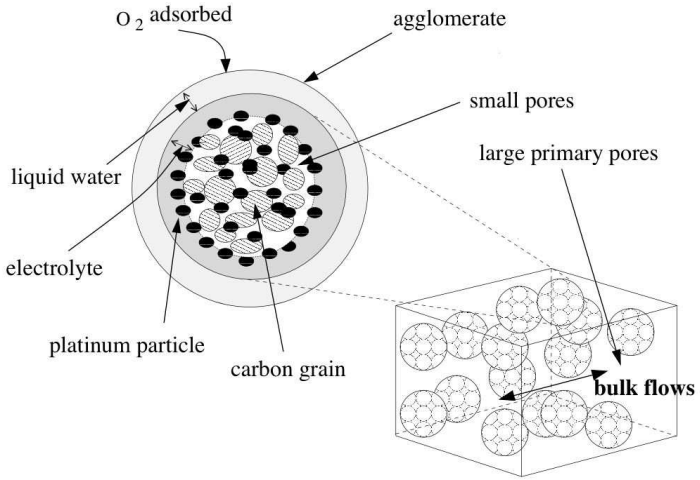

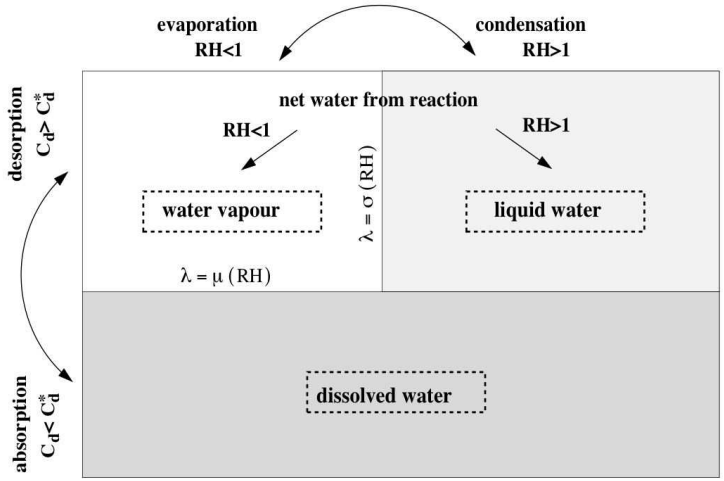

Gas: Oxygen in pore C_p, Oxygen dissolved in electrolyte C_e, Nitrogen C_N, Temp. T,

$$
\begin{aligned}
-\frac{d}{dy}\left(\epsilon_p(1-s)D_p\frac{dC_p}{dy}\right) &= -h_{pe}(1-s)(HC_p - C_e),\\
-\frac{d}{dy}\left(\epsilon_e D_e\frac{dC_e}{dy}\right) &= -\tfrac{1}{4}\mathcal{R}(\eta_c,T,C_e^s) + h_{ps}(1-s)(HC_p - C_e),\\
-\frac{d}{dy}\left(\epsilon_p(1-s)D_N\frac{dC_N}{dy}\right) &= 0,\\
-\frac{d}{dy}\left(k\frac{dT}{dy} - s\epsilon_p\rho_l C_L v_l T\right) &= \left(\frac{(-\delta s)T}{n_e} + F\eta\right)\mathcal{R}(\eta_c,T,C_e^s) +\\
&\quad +\epsilon_e\sigma_e\left(\frac{d\phi}{dy}\right)^2 + h_{gl}h_{pc}(RTC_v - P_{sat})
\end{aligned}
$$

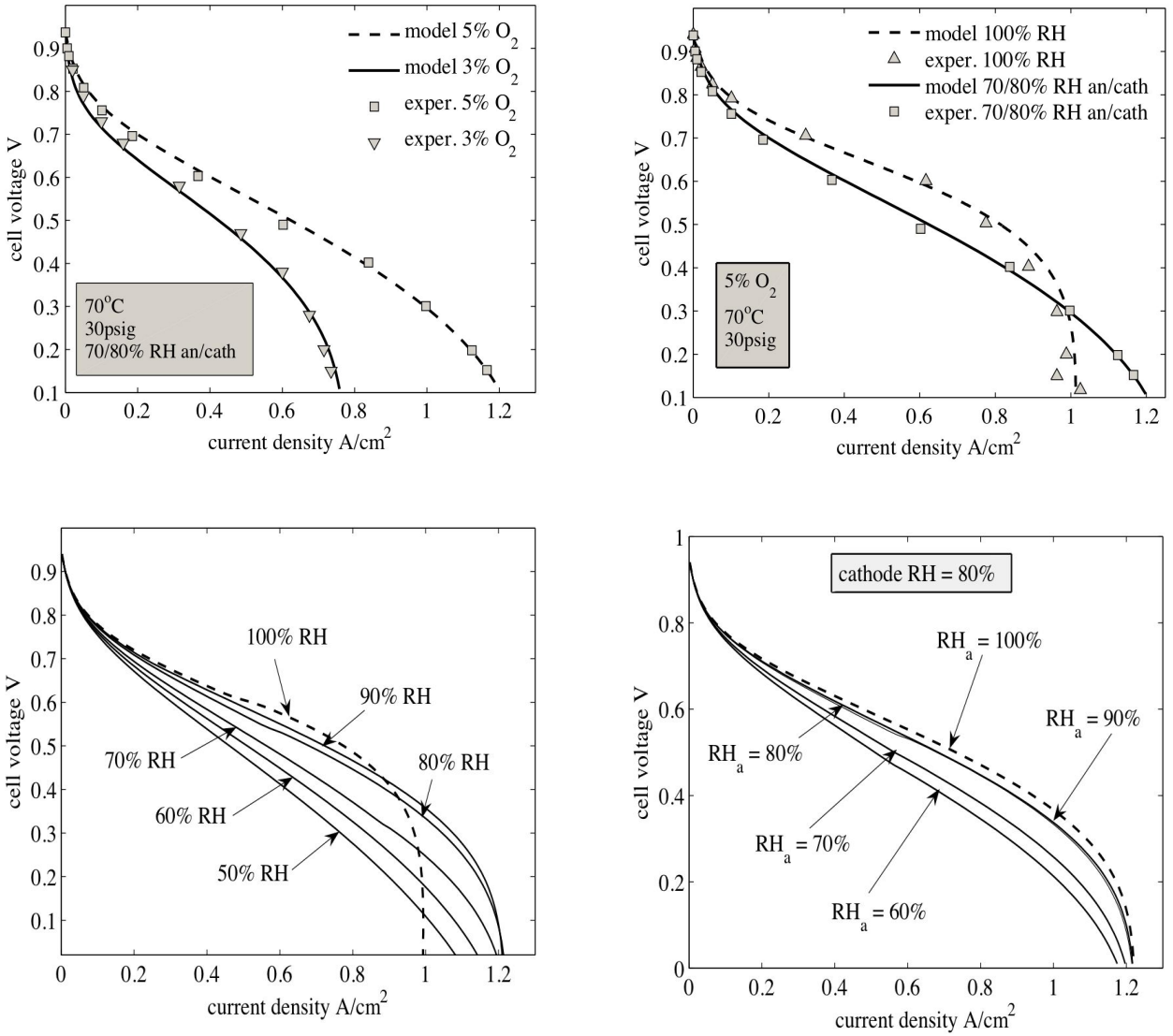

Polarization curves at (top left) Two different O_2 conc. (top right) two channel RHs (bottom left) 6 channel RHs with equal anode and cathode RH (bottom right) 5 anode RHs with cathode RH=80%

Nanophase Models

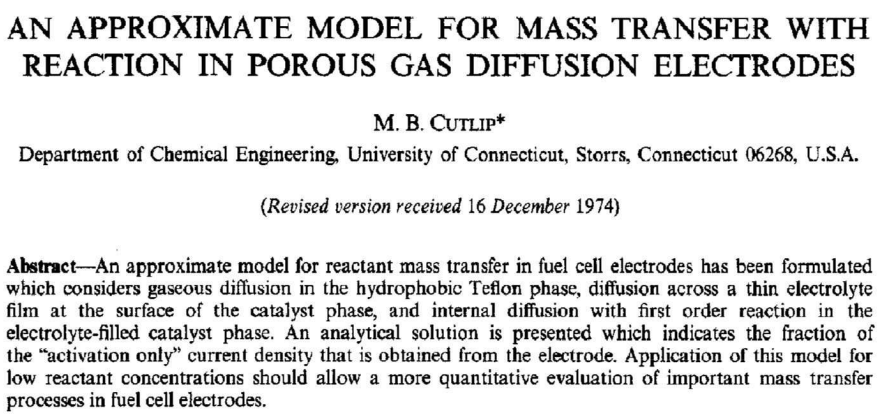

AN APPROXIMATE MODEL FOR MASS TRANSFER WITH REACTION IN POROUS GAS DIFFUSION ELECTRODES

M. B. CUTLIP*
Department of Chemical Engineering, University of Connecticut, Storrs, Connecticut 06268, U.S.A.

(*Revised version received* 16 *December* 1974)

Abstract—An approximate model for reactant mass transfer in fuel cell electrodes has been formulated which considers gaseous diffusion in the hydrophobic Teflon phase, diffusion across a thin electrolyte film at the surface of the catalyst phase, and internal diffusion with first order reaction in the electrolyte-filled catalyst phase. An analytical solution is presented which indicates the fraction of the "activation only" current density that is obtained from the electrode. Application of this model for low reactant concentrations should allow a more quantitative evaluation of important mass transfer processes in fuel cell electrodes.

Preparation Models: Resolve 5-50 nanometer scale of the ionomer/electrolyte and carbon support mixing process which fixes the catalyst nanoscale structure. Validate against SAX experiments (Andre Lee)

Performance Models: Determine the impact of the catalyst layer structure on heat and mass transport, including generation of liquid water regions and ionomer swelling

Degradation Models: Include additional reactions for carbon corrosion, Pt dissolution with accompanying phase change.

Follow ideas of C. Liu and N. Walkington, *Arch. Rat. Mech. Anal.*, **159** (2001) 229-252

In a 500 nanometer cube, track phase domains for carbon, ionomer, gas, liquid. Include interfacial energies (surface tension), van der Waals interactions, elastic energy, electrostatic interactions, to provide a force balance model for the mixing, phase change, transport and reaction which resolves down to the 5 nanometer length-scale.

Preparation Models

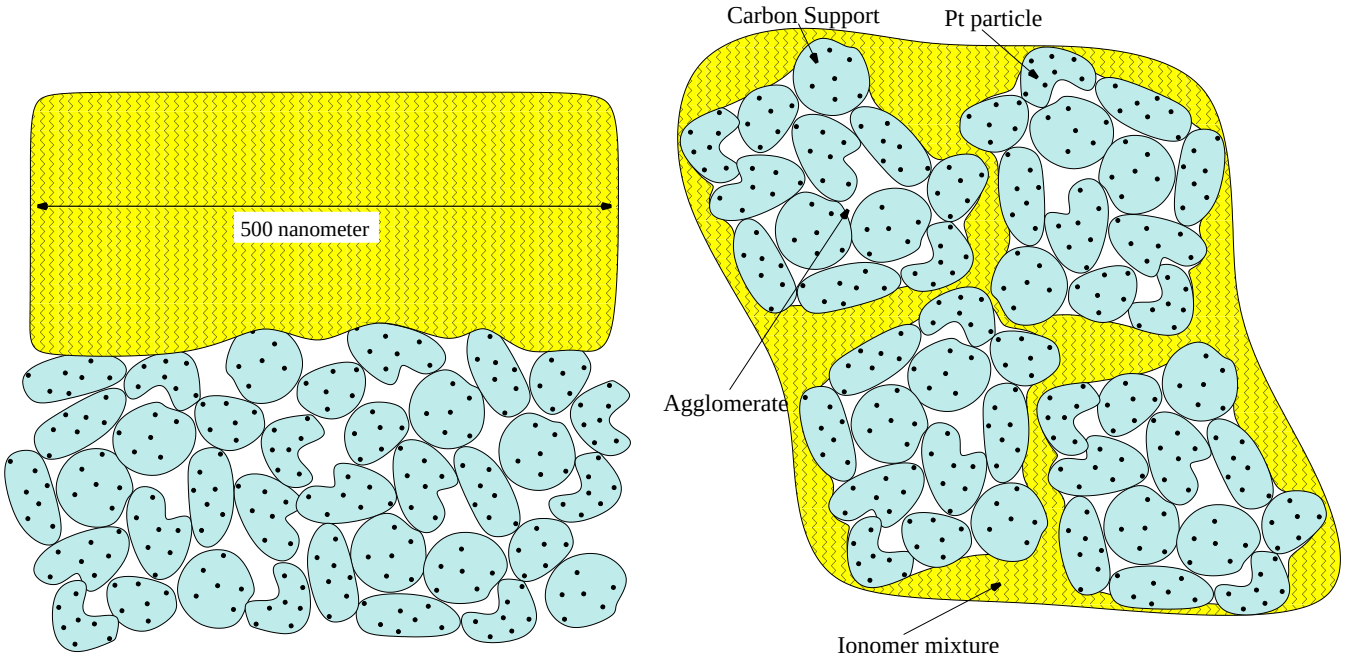

Carbon support is comprised of 30-40 nanometer carbon black particles with 5-10 nanometer Pt catalyst inclusions decorating the surface.

Carbon particulates naturally congregate into 150-250 nanometer agglomerates due to residual charges and surface interactions.

Agglomerated carbon is mixed with an aqueous polymer alcohol solution forming the catalyst ink.

How does surface wettability of carbon support/viscosity of polymer impact polymer interpenetration?

How should the external forces be optimized to mix “well”?

Preparation Model Details

Key Ideas:

Don't track interfaces Don't Impose BCs	Introduce a phase function ψ which takes three distinct values $\{\psi_s, \psi_i, \psi_g\} \subset \mathbf{R^2}$. to indicate whether $\psi(x)$ is solid, ionomer, or gas.
All Eulerian	Elastic deformation is naturally Lagrangian, but it can be pulled back into an Eulerian framework – write an *evolution* equation for the elastic deformation tensor.

Interfacial Energy

ϵ – interfacial length scale

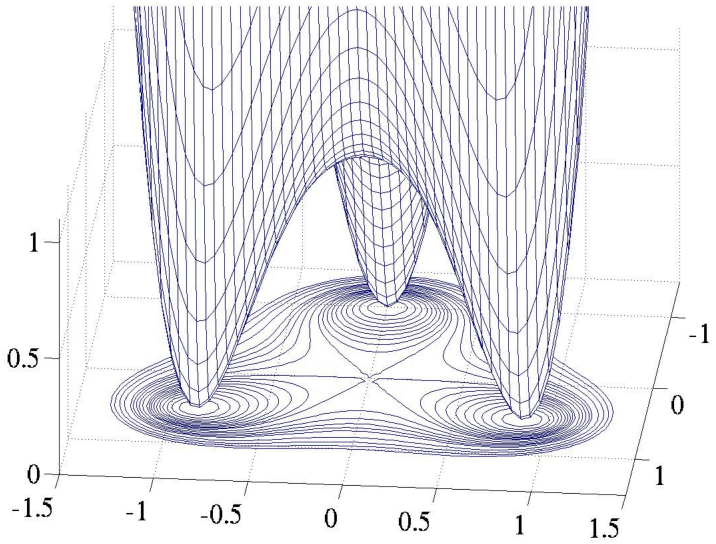

$$\psi_t + v.\nabla\psi = -\gamma\mathcal{G}\frac{\delta\mathcal{I}}{\delta\psi},$$

$$\nabla \cdot v = 0$$

$$\mathcal{I} = \int_\Omega \epsilon\left(|\nabla\psi|^2 + \frac{1}{\epsilon^2}W(\psi)\right)dx,$$

Inter-particle attractivity

Agglomeration driven by residual charges/weak surface bonding which we model with a van der Waals potential

$$\mathcal{N}(x) = \sum_{k \neq k_0}^{N_c} \left(\frac{\alpha}{(x_k - x)^M} - \frac{\beta}{(x - x_k)^N} \right)$$

where x_k is center of k'th carbon support and point x is inside particle k_0.

Force Balance for velocity

The mixture flows in response to body forces, elastic, interfacial, and electrostatic energy

$$\rho(v_t + v.\nabla v) + \nabla \pi = \nabla \cdot (\mu(\psi) D v) + \frac{\delta \mathcal{I}_\epsilon}{\delta \psi_\epsilon} \nabla \psi_\epsilon + \chi_s \left(\nabla \cdot (\mathcal{D} \mathcal{W}(F) F^T) + \nabla \mathcal{N} \right) + \rho f$$

Body force driving mixing	f
Indicator function for phase p	χ_p
Pressure	π, conjugate to incompressibility
Density	$\rho = \rho_s \chi_s(x) + \rho_i \chi_i(x) + \rho_g \chi_g(x)$
Viscosity	$\mu = \mu_s \chi_s(x) + \mu_i \chi_i(x) + \mu_g \chi_g(x)$

High Temperature PEM Fuel Cells: Baker Group

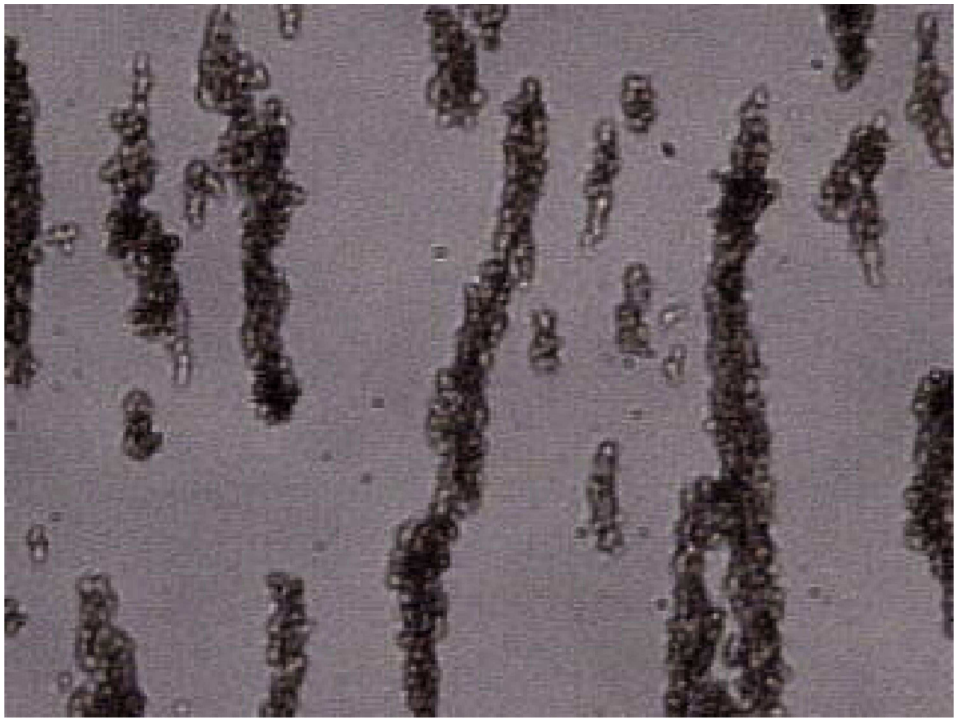

- Sulfonic acid-containing nanoparticles can be assembled into ion-conducting networks within hydrophobic polymers, with the resulting composites having conductivities and mechanical properties as good as, or superior to Nafion.
- Develop new fuel cell membrane materials with the mechanical properties and conductivity consistent with high temperature operation.
- The two-phase approach to membrane design promises to dramatically reduce the cost of membrane manufacturing costs, since the particles and the hydrophobic polymer can be independently optimized.

Pt dissolution

Two principle mechanisms for Platinum loss in the catalyst layer have been proposed: surface migration and Pt dissolution/reprecipitation.

Patterson [2002] suggests that Pt dissolution is a major source of Pt surface area loss.

Yasuda [2006] has shown that potential cycling can induce Pt dissolution, that rates of dissolution are greatly impacted by molecular hydrogen concentrations, and the location of Pt deposits moves towards the anode with reduction of hydrogen concentration in the membrane

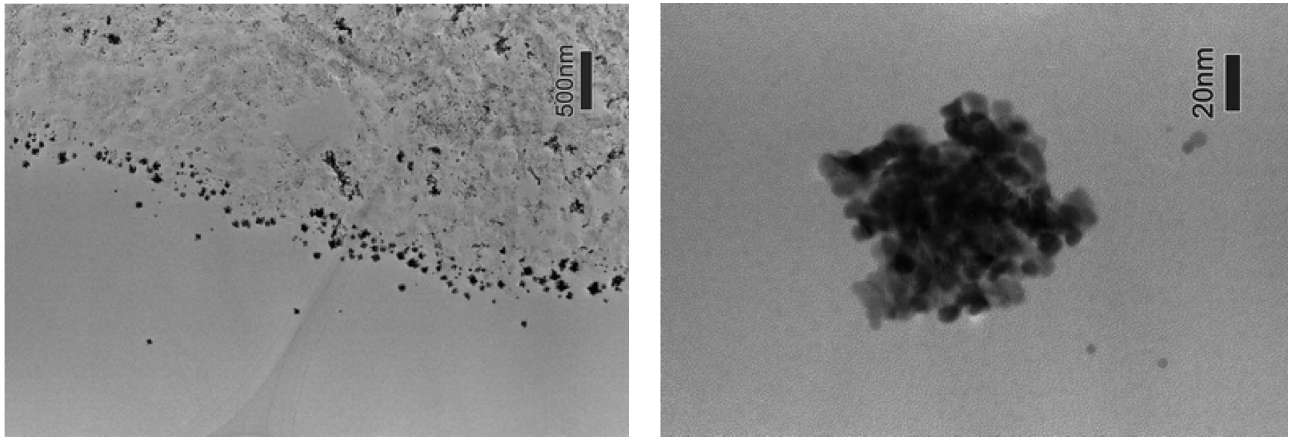

(Left) A TEM image of the interface between the cathode catalyst layer and the polymer electrolyte membrane of an MEA after a potential cycling test for 500 cycles under a nitrogen atmosphere (sample N-5). Potential cycling range: 0.1-1.2 V vs. SHE. (Right) Enlargement of deposited Pt particles. From Yasuda et al [2006].

Include extra phase for Pt metal, and extra reactions

$$\mathbf{Pt + H_2O \rightleftharpoons PtO + 2H^+ + 2e^-}$$

$$\mathbf{PtO + 2H^+ \rightleftharpoons Pt^{2+} + H_2O}$$